Annexure I

Name of sampling points and their locations

Anand District

S. N.	Location name	Latitude	Longitude
1.	Gambhira	22°19'40.94	72°51'20.41
2.	Bilpad	22°18'42.96	72°58'35.69
3.	Anklav	22°22'36.51	72°00'02.20
4.	Asodar	22°25'25.10	72°59'38.25
5.	Napad-talpad	22°28'40.20	72°59'30.38
6.	Napa-vanto	22°28'25.54	72°55'36.35
7.	Agas	22°29'28.71	72°52'53.24
8.	Porda	22°32'05.07	72°49'39.41
9.	Ravli	22°34'05.07	72°51'23.43
10.	Lambhvel	22° 34.974	72° 56.033'
11.	Samarkha	22° 36.086	72° 59.082
12.	Kasor	22° 32.325	72° 54.746
13.	Jakhala	22° 39.467	73° 02.934
14.	Gangapura	22° 39.524	73° 05.185
15.	Ghora	22° 42.426	73° 02.873
16.	Vansol	22° 41.207	73° 00.314
17.	Umreth	22° 41.964	73° 06.690
18.	Khambloj	22° 34.434	73° 04.995
19.	Moti sherdi	22° 19.875	72° 56.961
20.	Kosindra	22° 22.386	72° 58.633
21.	Khadol	22° 19.886	72° 56.946
22.	Amrol	22° 22.519	73° 02.486
23.	Bhetasi	22° 25.145	73° 02.292
24.	Adas	22° 28.805	73° 01.903
25.	Gopalpura	22° 31.526	72° 59.577
26.	Bedva	22° 33.170	73° 02.155
27.	Pamol	22° 26.694	72° 56.546
28.	Vahera	22° 25.452	72° 53.094
29.	Kasari	22° 23.064	72° 52.753
30.	Umlav	22° 18.543	72° 52.778
31.	Kankapura	22° 16.641	72° 49.120
32.	Khadodhi	22° 16.470	72° 45.968
33.	Kandhroti	22° 19.599	72° 46.560
34.	Divel	22° 18.874'	72° 48.475'
35.	Saijpur	22° 21.825'	72° 49.025'
36.	Sundarna	22° 25.738'	72° 49.073'
37.	Danteli	22° 25.735'	72° 49.063'
38.	Jahaj	22° 21.993'	72° 44.294'
39.	Piploi	22° 22.251'	72° 42.160'
40	Bhuvel	22° 19.513'	72° 42.921'
41	Rajpur	22° 17.323'	72° 41.554'
42	Shakarpur	22° 18.965'	72° 38.220'
43	Kodva	22° 23.140'	72° 38.319'
44	Paldi	22° 21.902'	72° 34.518'
45	Hasanpura	22° 22.975'	72° 30.077'
46	Rohni	22° 24.971'	72° 28.423'
47	Mitli	22° 25.060'	72° 23.842'
48	Golana	22° 27.470'	72° 25.255'
49	Navagambara	22° 20.937'	72° 29.860'
50	Vainaj	22° 20.527'	72° 28.015'
51	Pandad	22° 22.604'	72° 27.176'
52	Tarakpur	22° 22.612'	72° 25.744'
53	Galiyana	22° 30.296'	72° 26.398'

54	Chitarwada	22° 32.220'	72° 27.741'
55	Nabhoi	22° 33.898'	72° 27.438'
56	Mota kalodra	22° 35.735'	72° 29.974'
57	Kanavada	22° 33.144'	72° 32.130'
58	Ishanpur	22° 28.735'	72° 32.061'
59	Bhudhej	22° 26.090'	72° 35.595'
60	Jafrabad	22° 25.382'	72° 31.968'
61	Tarapur	22° 28.897'	72° 39.766'
62	Chikhaliya	22° 28.214'	72° 35.209'
63	Bhanderaj	22° 25.596'	72° 38.551'
64	Nar	22° 28.429'	72° 42.289'
65	Manpura	22° 26.306'	72° 41.667'
66	Amod	22° 29.357'	72° 44.625'
67	Dantali	22° 28.564'	72° 49.256'
68	Changa	22° 35.502'	72° 48.135'
69	Ramol	22° 37.874'	72° 47.482'
70	Run	22° 37.641'	72° 45.631'
71	Petli	22° 35.841'	72° 45.371'
72	Bhadkhad	22° 37.185'	72° 42.269'
73	Bantawa	22° 36.405'	72° 41.387'
74	Devataj	22° 32.263'	72° 42.239'
75	Isnav	22° 31.864'	72° 45.287'
76	Bakrol	22° 33.959'	72° 54.587'
77	Kunjrao	22° 35.927'	73° 02.836'
78	Khanpur	22° 32.158'	73° 08.163'
79	Shili	22° 35.796'	73° 08.334'
80	Bharoda	22° 37.631'	73° 08.247'
81	Bhatpura	22° 41.051'	73° 09.110'
82	Gajana	22° 16.660'	72° 54.064'

Vadodara District

S. N.	Location name	Latitude	Longitude
1	Mangrej	22° 05.000'	73° 10.759'
2	Ganpatpura	22° 03.622'	73° 11.432'
3	Nishaliya	22°59.547	73°11.756
4	Kanthariya	21° 57.054'	73° 11.550'
5	Hirjipura	21° 53.591'	73° 13.276'
6	Lilod	21° 52.662'	73° 13.747'
7	Motikoral	21° 49.977'	73° 12.500'
8	Saring	21° 53.583'	73° 07.415'
9	Mantroj	21° 53.175'	73° 05.931'
10	Sarupur	21° 55.585'	73° 08.531'
11	Kothia	21° 56.196'	73° 14.518'
12	Lokadra	21° 59.389'	73° 06.379'
13	Valan	21° 57.324'	73° 04.343'
14	Dhamanja	21° 59.755'	73° 04.340'
15	Miyagam navi nagari	22°01.971'	73°05.342'
16	Mangrol	22° 00.506'	73° 02.274'
17	Bodka	22°02.937'	73°01.746'
18	Abhara	22° 05.201'	73° 00.472'
19	Manpur	22° 06.172'	73° 04.075'
20	Kherda	22° 05.994'	73° 08.121'
21	Juni jithardi	22° 02.190'	73° 08.563'
22	Gutaj	22° 22.186'	73° 38.998'
23	Goraj	22° 20.085	73° 29.117
24	Rustampura	22° 17.007'	73° 32.352'
25	Vedpur	22° 19.697'	73° 31.415'
26	Gugalpura	22° 16.239'	73° 27.945'
27	Karamaliyapura	22° 13.699'	73° 26.141'

28	Tavra	22° 17.520'	73° 24.818'
29	Madhodar	22° 18.969'	73° 25.005'
30	Khandha	22° 19.399'	73° 22.551'
31	Limda	22° 17.025'	73° 21.867'
32	Umarva	22° 16.479'	73° 18.701'
33	Navi jambuvai	22° 20.175'	73° 18.759'
34	Bhaniyara	22° 23.359'	73° 16.104
35	Lilora	22° 26.520'	73° 21.596'
36	Kotambi	22° 23.741'	73° 18.568'
37	Fajalpur	22° 25.815'	73° 04.497'
38	Sankarda	22° 25.783'	73° 07.321'
39	Bajwa	22° 22.130'	73° 08.385'
40	Anagadh	22° 23.367'	73° 05.053'
42	Bhayali	22° 16.963'	73° 07.523'
43	Itola	22° 08.615'	73° 08.696'
44	Por	22° 08.533'	73° 11.180'
45	Salad	22° 08.680'	73° 14.472'
46	Alhadpura	22° 13.773'	73° 15.421'
47	Kapurai	22° 16.131'	73° 15.178'
48	Mujar gamdi	22° 13.107'	73° 12.319'
49	Sayajipura	22° 19.675'	73° 15.349'
50	Dumad	22° 22.452'	73° 11.371'
51	Sindhrot	22° 19.867'	73° 03.611'
52	Shanpur	22° 06.670'	72° 57.533'
53	Umaj	22° 04.136'	72° 57.910'
54	Abhol	22° 07.182'	72° 54.502'
55	Masar	22° 07.182'	72° 54.502
56	Gavasad	22° 09.604'	72° 56.679'
57	Karkhadi	22° 12.483'	72° 54.283'
58	Somjipura	22° 12.810'	72° 58.022'
59	Sultanpura	22° 15.439'	72° 56.760
60	Ekalbara	22° 15.430'	73° 00.619'
61	Ranu	22° 12.667'	73° 01.432'
62	Rajupura	22° 10.064'	73° 00.565'
63	Amla	22° 10.337	73° 04.466
64	Ghayaj	22° 12.932'	73° 05.386'
65	Tajpura	22° 15.589'	73° 04.173'
66	Patod	22° 13.111'	73° 07.112'
67	Gotri	22° 18.883'	73° 07.999'
68	Dabhoigam	22° 07.935'	73° 24.880'
69	Gamdi	22° 05.657'	73° 24.276'
70	Tentalav	22° 05.657'	73° 24.276'
71	Akoti	22° 02.980'	73° 28.530'
72	Asgol	22° 04.115'	73° 31.420'
73	Juni mangrol	22° 05.729'	73° 28.276'
74	Habipura	22° 06.194'	73° 21.440'
75	Kothara	22° 06.216'	73° 18.266'
76	Kunvapura (kuvarpura)	22° 05.988'	73° 16.063'
77	Lingasthali	22° 03.094'	73° 15.085'
78	Angusthan	22° 09.938'	73° 18.366'
79	Puda	22° 10.286'	73° 22.582'
80	Tarsana	22° 09.448'	73° 24.793'
81	Vadhvana	22° 09.292'	73° 29.375'
82	Kanteshwar	22° 12.698'	73° 30.065'
83	Kaddhara	22° 12.210'	73° 22.490'
84	Palaswada	22° 12.210'	73° 22.490'
85	Barkal	21° 56.235'	73° 24.905'
86	Kanjetha	21° 55.929'	73° 21.534'
87	Malsar	21° 53.451'	73° 18.706'
88	Sursamar (sursamal)	21° 55.989'	73° 17.863'
89	Sadhli	21° 58.988'	73° 17.501'

90	Tinglod	21° 59.555'	73° 14.873'
91	Garadi	22° 02.935'	73° 18.185'
92	Simli	21° 59.239'	73° 21.920'
93	Satishana	22° 00.155'	73° 24.721'
94	Puniyad	22° 02.376'	73° 21.741'
95	Jafarapura	22° 23.664'	73° 22.071'
96	Kheda karmasiya	22° 25.224'	73° 24.100'
97	Adiran	22° 26.694'	73° 24.744'
98	Rajpura	22° 29.992'	73° 24.388'
99	Khakhariya	22° 32.310'	73° 24.458'
100	Lotna	22° 29.990'	73° 21.916'
101	Tulsipura	22° 34.113'	73° 22.249'
102	Dantej (dhantej)	22° 35.868'	73° 21.530'
103	Gorsan	22° 39.762'	73° 18.050'
104	Desar	22° 43.017'	73° 17.445'
105	Intvad	22° 43.317'	73° 15.838'
106	Waghpura	22° 45.633'	73° 15.619'
107	Jambugoral	22° 46.486'	73° 19.489'
108	Vejpur	22° 44.338'	73° 21.289'
109	Tulsigam	22° 46.959'	73° 23.360'
110	Namisara	22° 30.120'	73° 11.063'
111	Manjusar	22° 26.679'	73° 11.418'
112	Pandu	22° 40.247'	73° 22.254'
113	Mokampura	22° 40.590'	73° 24.503'
114	Vitoj	22° 37.343'	73° 18.069'
115	Raswadi	22° 36.513'	73° 14.372'
116	Rupankui	22° 35.520'	73° 12.640'
117	Sardarpura	22° 33.413'	73° 11.368'
118	Javla	22° 33.462'	73° 14.015'
119	Charanpura	22° 33.961'	73° 17.325'
120	Pratapnagar (khaneravpura)	22° 29.623'	73° 17.674'
121	Garadhia	22° 27.553'	73° 19.000'
122	Pasva	22° 30.045'	73° 15.210'
123	Alindra	22° 26.801'	73° 13.912'
124	Raniya	22° 29.911'	73° 07.602'
125	Jalampura	22° 29.552'	73° 05.667'
126	Nizampura	22° 20.270'	73° 11.299'
127	Station	22° 18.609'	73° 10.838'

Bharuch District

S. N.	Location name	Latitude	Longitude
1	Nada	N21° 57.135'	E72° 33.704'
2	Asarsa	N21° 57.092'	E72° 35.527'
3	Devla	N21° 59.771'	E72° 34.588'
4	Malpor	N22° 02.788'	E72° 33.834'
5	Kansagar	N22° 02.363'	E72° 37.836'
6	Thakor talawadi	N21° 59.338'	E72° 37.386'
7	Tankari	N21° 59.473'	E72° 40.452'
8	Chandpor bara	N22° 02.131'	E72° 41.518'
9	Jantran	N22° 05.816'	E72° 38.633'
10	Zamdi	N22° 06.562'	E72° 34.917'
11	Dahegam	N22° 11.165'	E72° 35.487'
12	Kavi	N22° 11.678'	E72° 38.371'
13	Runad	N22° 08.735'	E72° 38.932'
14	Uchchhad	N22° 05.626'	E72° 52.282'
15	Jambusar	N22° 04.380'	E72° 48.059'
16	Limaj	N22° 03.577'	E72° 45.581'
17	Kora	N22° 06.785'	E72° 41.384'
18	Kavli	N22° 08.114'	E72° 42.757'

19	Amanpor nana	N22° 07.400'	E72° 44.823'
20	Bhador	N22° 06.177'	E72° 44.781'
21	Uber	N22° 07.736'	E72° 48.174'
22	Vedach	N22° 08.656'	E72° 50.180'
23	Dhaba	N22° 06.230'	E72° 49.230'
24	Piludra	N22° 09.790'	E72° 51.293'
25	Kahanva	N22° 10.629'	E72° 54.479'
26	Kareli	N22° 11.854'	E72° 52.006'
27	Bhimpura	N21° 59.280'	E72° 52.539'
28	Junawadiya	N22° 02.290'	E72° 53.281'
29	Pursa	N21° 59.795'	E72° 49.248'
30	Valipor	N21° 56.342'	E72° 45.050'
31	Denva	N21° 56.446'	E72° 44.230'
32	Intola	N21° 55.840'	E72° 49.832'
33	Bodka	N21° 55.964'	E72° 53.033'
34	Anor	N21° 55.772'	E72° 55.598'
35	Samni	N21° 52.147'	E72° 55.500'
36	Dora	N21° 57.085'	E72° 59.516'
37	Sarbhan	N21° 59.473'	E72° 56.767'
38	Kobla	N22° 02.617'	E72° 56.327'
39	Matar	N22° 00.330'	E72° 59.501'
40	Ochchhan	N21° 59.373'	E73° 01.811'
41	Kharetha	N21° 41.934'	E73° 27.541'
42	Haldarwa	N21° 45.760'	E73° 02.500'
43	Mangleshwar	N21° 45.876'	E73° 07.821'
44	Jhadeshwar	N21° 40.610'	E72° 34.438'
45	Rahadpor	N21° 41.336'	E72° 33.239'
46	Manubar	N21° 45.991'	E72° 38.627'
47	Vesdada	N21° 47.969'	E72° 38.259'
48	Kasva	N21° 52.145'	E72° 41.540'
49	Sankhwad	N21° 49.207'	E72° 41.551'
50	Vilayat	N21° 47.019'	E72° 41.796'
51	Derol	N21° 53.008'	E72° 45.666'
52	Kelod	N21° 51.845'	E72° 48.024'
53	Padariya	N21° 41.902'	E73° 06.620'
54	Pariej	N21° 43.136'	E73° 08.083'
55	Paguthan	N21° 39.711'	E73° 12.865'
56	Sayakha	N21° 39.415'	E73° 10.380'
57	Sadathala	N21° 42.920'	E73° 14.351'
58	Bhansali	N21° 45.973'	E73° 13.131'
59	Atali	N21° 49.119'	E73° 12.633'
60	Jolva	N21° 49.038'	E73° 11.593'
61	Dahej	N21° 49.038'	E73° 11.593'
61	Jageshwar	N21° 49.511'	E73° 05.782'
63	Lakhigam	N21° 51.872'	E73° 06.676'
64	Kadodara	N21° 47.198'	E73° 22.001'
65	Paniadara	N21° 46.755'	E73° 20.041'
66	Muler	N21° 42.142'	E73° 23.529'
67	Ambhel	N21° 40.610'	E72° 34.438'
68	Nadarkha	N21° 41.336'	E72° 33.239'
69	Badalpura	N21° 45.991'	E72° 38.627'
70	Pahaj	N21° 47.969'	E72° 38.259'
71	Nana sanja	N21° 52.145'	E72° 41.540'
72	Mota sanja	N21° 49.207'	E72° 41.551'
73	Moran	N21° 47.019'	E72° 41.796'
74	Navagam mota	N21° 53.008'	E72° 45.666'
75	Amod	N21° 51.845'	E72° 48.024'
76	Madhavpara	N21° 41.902'	E73° 06.620'
77	Krushnapuri	N21° 43.136'	E73° 08.083'
78	Bhalod	N21° 39.711'	E73° 12.865'
79	Juna pora	N21° 39.415'	E73° 10.380'

80	Samlod	N21° 42.920'	E73° 14.351'
81	Shahpura	N21° 45.973'	E73° 13.131'
82	Kesharva	N21° 49.119'	E73° 12.633'
83	Vali	N21° 49.038'	E73° 11.593'
84	Mungaj	N21° 49.038'	E73° 11.593'
85	Timla	N21° 39.712'	E73° 23.497'
86	Galiba	N21° 39.642'	E73° 27.178'
87	Kakarkui	N21° 35.759'	E73° 26.890'
88	Baladawa	N21° 36.251'	E73° 23.400'
89	Kavachia	N21° 31.925'	E73° 21.405'
90	Mirapor	N21° 30.347'	E73° 20.169'
91	Kamaliya	N21° 34.034'	E73° 20.424'
92	Sakkapor	N21° 38.688'	E72° 55.241'
93	Matied	N21° 37.190'	E72° 52.910'
94	Mothiya	N21° 36.294'	E72° 51.522'
95	Utraj	N21° 35.282'	E72° 49.529'
96	Alva	N21° 33.102'	E72° 49.170'
97	Vansholi	N21° 33.048'	E72° 46.390'
98	Jetpor	N21° 29.108'	E72° 42.385'
99	Dhamrad	N21° 29.655'	E72° 46.087'
100	Aniyadara	N21° 29.861'	E72° 48.530'
101	Sahol	N21° 26.502'	E72° 49.230'
102	Panjroli	N21° 27.179'	E72° 53.650'
103	Sisodara	N21° 30.176'	E72° 53.429'
104	Mahuvada	N21° 49.811'	E73° 19.471'
105	Asha	N21° 53.256'	E73° 17.737'
106	Nana vasna	N21° 53.477'	E73° 14.211'
107	Mota vasna	N21° 55.470'	E73° 14.820'
108	Rumalpura	N21° 49.712'	E73° 16.554'
109	Rupania	N21° 46.070'	E73° 16.559'
110	Razalwada	N21° 43.320'	E73° 18.375'
111	Jamoli	N21° 43.150'	E73° 20.108'
112	Kuri	N21° 39.917'	E73° 20.268'
113	Kothiyamau	N21° 39.914'	E73° 17.061'
114	Bedoli	N21° 37.274'	E73° 20.319'
115	Singalvan	N21° 36.684'	E73° 17.697'
116	Vaghalkhod	N21° 35.588'	E73° 12.754'
117	Valia	N21° 34.337'	E73° 09.643'
118	Jamania	N21° 35.179'	E73° 10.785'
119	Dholgam	N21° 35.982'	E73° 10.342'
120	Umargam	N21° 32.402'	E73° 13.064'
121	Bharadiya	N21° 30.534'	E73° 14.685'
122	Dansoli	N21° 30.175'	E73° 09.488'
123	Joli	N21° 30.215'	E73° 06.756'
124	Kanerav	N21° 33.017'	E73° 09.570'
125	Survani	N21° 38.723'	E73° 00.170'
126	Nangal	N21° 36.677'	E72° 55.274'
127	Rohid	N21° 32.142'	E72° 51.888'
128	Uthiyadara	N21° 29.358'	E72° 56.766'
129	Alonj	N21° 33.235'	E72° 57.279'
130	Sanjali	N21° 33.298'	E72° 59.628'
131	Kapodara	N21° 35.627'	E73° 00.475'
132	Bhadi	N21° 33.007'	E73° 01.799'
133	Bharan	N21° 30.466'	E73° 02.376'
134	Dodwada	N21° 32.389'	E73° 05.782'
135	Piprod	N21° 36.748'	E73° 05.912'
136	Jitali	N21° 37.169'	E73° 03.881'
137	Kharchi	N21° 40.129'	E73° 05.376'
138	Motali	N21° 39.066'	E73° 02.630'
139	Ankot	N21° 49.104'	E72° 52.799'
140	Pisad	N21° 49.873'	E72° 49.241'

141	Ora	N21° 52.231'	E72° 52.717'
142	Kargat	N21° 49.660'	E73° 02.530'
143	Ghodi	N21° 53.127'	E73° 02.318'
144	Simaliya	N21° 55.137'	E73° 02.617'

Narmada District

S.N.	Location name	Latitude	Longitude
1	Panchpipri	N21°30.006	E73°48.375
2	Parodhi	N21°29.812	E73°51.980
3	Kolvan	N21°30.473	E73°55.848
4	Chatuvad	N21°30.033	E73°57.754
5	Amiyar	N21°33.232	E73°45.133
6	Gopal pura	N21°51.765	E73°33.799
7	Motiraval	N21°52.294	E73°38.092
8	Kevadiya	N21°52.946	E73°42.286
9	Panisadadia	N21°58.092	E73°43.767
10	Undava	N21°55.857	E73°44.590
11	Vaghrali	N21°55.201	E73°47.562
12	Limkhetar	N21°54.815	E73°50.953
13	Arethi	N21°36'42.88	E73˚26'28.51
14	Khatam	N21°39'28.97	E73˚38'19.76
15	Sankali	N21°42'10.11	E73˚43'56.36
16	Dumkhal	N21°44'37.88	E73˚50'17.20
17	Kokam	N21°44'07.28	E73˚49'28.88
18	Vanzar	N21°50'10.38	E73˚30'56.25
19	Mota raypara	N21°52'12.38	E73˚41'56.68
20	Devmogra	N21° 35.690'	E73° 42.913'
21	Devidav	N21° 35.903'	E73° 47.668'
22	Ghansera	N21° 32.232'	E73° 48.578'
23	Bodvav	N21° 29.609'	E73° 44.734'
24	Padi	N21° 25.719'	E73° 42.022'
25	Motakakdi amba	N21° 26.699'	E73° 45.142'
26	Samot	N21° 39.281'	E73° 51.324'
27	Kelda	N21° 39.317'	E73° 48.743'
28	Juna mosda	N21° 41.454'	E73° 42.418'
29	Mediasag (medyusag)	N21° 35.954'	E73° 38.563'
30	Katipani(kantipani)	N21° 32.788'	E73° 41.436'
31	Kamodhvav	N21° 30.261'	E73° 40.168'
32	Indlavi	N21° 29.284'	E73° 37.264'
33	Moskut	N21° 29.868'	E73° 34.106'
34	Rojghat	N21° 30.041'	E73° 31.815'
35	Rodha	N21° 33.422'	E73° 31.153'
36	Mulkapada	N21° 32.574'	E73° 33.362'
37	Garda	N21° 32.556'	E73° 33.359'
38	Jambar	N21° 36.444'	E73° 31.142'
39	Nivalda	N21° 37.413'	E73° 35.044'
40	Bore	N21° 39.010'	E73° 34.434'
41	Fulsar	N21° 42.400'	E73° 35.315'
42	Kabripathar	N21° 41.946'	E73° 32.691'
43	Kanjal	N21° 45.472'	E73° 34.786'
44	Duthar	N21° 42.628'	E73° 37.525'
45	Morjadi	N21° 38.477'	E73° 45.621'
46	Kumbhkhadi	N21° 33.149'	E73° 38.236'
47	Poicha	N21° 33.149'	E73° 38.236'
48	Guvar	N21° 55.533'	E73° 34.554'
49	Anodara	N21° 55.591'	E73° 31.724'
50	Rundh	N21° 56.655'	E73° 27.408'
51	Rajpipla (m)	N21° 51.750'	E73° 30.809'
52	Dholivav	N21° 52.243'	E73° 27.267'

53	Ori	N21° 54.643'	E73° 23.504'
54	Amarpara	N21° 52.273'	E73° 24.283'
55	Rajpara(rajupura)	N21° 52.093'	E73° 20.044'
56	Rajuvadia	N21° 50.705'	E73° 20.643'
57	Khojalvasa	N21° 49.743'	E73° 24.007'
58	Nanahaidva	N21° 50.225'	E73° 27.953'
59	Namalgadh	N21° 44.490'	E73° 25.592'
60	Moji	N21° 43.412'	E73° 27.503'
61	Mandan	N21° 45.772'	E73° 29.922'
62	Chhatwada (dhatwada)	N21° 47.106'	E73° 25.160'
63	Dadhvada	N21° 46.224'	E73° 26.775'
64	Bhilvashi	N21° 51.393'	E73° 39.047'
65	Zarnavadi(zarvani)	N21° 48.306'	E73° 42.214'
66	Thavadiya	N21° 49.784'	E73° 42.680'
67	Mokhadi	N21° 49.264'	E73° 44.828'
68	Survani	N21° 53.312'	E73° 47.946'
69	Gadher	N21° 53.485'	E73° 50.140'
70	Maunipada	N21° 26.686'	E73° 46.150'
71	Vandri	N21° 46.592'	E73° 48.132'
72	Mathasar	N21° 47.188'	E73° 47.440'
73	Moriya	N21° 58.983'	E73° 31.744'
74	Naliya	N21° 58.914'	E73° 34.084'
75	Vandh	N21° 58.812'	E73° 37.103'
76	Vyadhar	N21° 55.982'	E73° 40.114'
77	Dhanikod	N21° 56.236'	E73° 38.394'
78	Shira	N21° 59.704'	E73° 40.483'
79	Agar	N22° 01.863'	E73° 39.568'
80	Amaliya	N22° 02.131'	E73° 37.849'
81	Undai mandva	N22° 02.411'	E73° 33.459'
82	Fatepur	N22° 01.642'	E73° 33.783'
83	Jalodara	N22° 02.738'	E73° 31.828'
84	Bantawadi	N21° 37.722'	E73° 41.393'
85	Sejpur	N21° 36.074'	E73° 29.192'
86	Dhanor	N21° 38.755'	E73° 30.241'
87	Naghatpor	N21° 53.281'	E73° 46.051'

PUBLICATIONS

- **Patel D**, Pamidimukkala P, Chakraborty D. Groundwater quality evaluation of Narmada district, Gujarat using principal component analysis. *Groundwater for Sustainable Development*, 2024.
- **Patel D**, Jindal MK, Pamidimukkala PS, Chakraborty D. Gamma radiation dose rate distribution in the Anand, Bharuch, Vadodara, and Narmada districts of Gujarat, India. *Environmental Science and Pollution Research*, 2023
- **Patel D**, Pamidimukkala P, Chakraborty D, Yadav A. Bharuch District, Gujarat, India: Factor analysis and geographical distribution of water quality characteristics. *Environmental Nanotechnology, Monitoring & Management*. 2022

PAPER PRESENTED

- Poster presentation on 'Pre- and Post-monsoon variation of uranium and associated water quality parameters in Narmada district of Gujarat', Twentieth National Symposium on Environment (NSE-20), IIT-Gandhinagar, 13-15th Dec 2018.
- Poster presentation on 'Spatial Distribution of Uranium in drinking water of Tilakwada Tehsil and its removal using chitosan-based derivative', National Symposium on Advance in Chemical Research (ACR-2019), MSU, Baroda, Vadodara, 24th Feb 2019.
- Oral presentation on 'Monitoring of uranium and fluoride in drinking water of Bharuch district of Gujarat', National seminar on Interdisciplinary Approaches in Environmental Sciences (IAES-01), MSU, Baroda, Vadodara, 18-19th Jan 2020.
- Oral presentation on 'Monitoring of fluoride along with some physico-chemical parameters in Anand, Vadodara, and Bharuch districts of Gujarat state', International

Conference on Ecohealth and Environmental Sustainability (ICEES-2020), Navrachana University, Vadodara, 24-26th Feb 2020.

- Poster presentation on ‘Spatial distribution of uranium and fluoride in groundwater sources of Anand district in Gujarat’, India, International conference on technologies for smart green connected societies 2021, ICTSGS, SPAST Foundation, Kerala, 29th-30th Nov, 2021.
- Oral presentation on ‘Terrestrial Radiation Dose Rate Distribution in the Four Districts of Gujarat, India, International Conference on Radiation Awareness and Detection in Natural Environment’, Dolphin (PG) Institute of Biomedical and Natural Sciences, Dehradun, 2nd – 4th March 2023.

CONFERENCE AND WORKSHOP ATTENDED

- National Conference on National conference on pollution management NCPM-2018, MSU, Baroda, 3rd Feb 2018.
- 5th National Uranium Project (NUP) Workshop on Statistical Analysis of Data Generated Under National Uranium Project at Bhabha Atomic Research Centre (BARC), Mumbai-2018, BARC, Mumbai, 26-27th Sept 2018.
- Indian Society of Analytical Scientists’ seminar, MSU, Baroda, 9th March 2019.
- One-day seminar on analytical instrumental techniques, MSU, Baroda, 9th March 2019
- Indus synchrotrons user’s meeting (ISUM), UGC-DAE CSR, Indore, 27-29th March 2019.
- One-day seminar on Environmental Impact Assessment, MSU, Baroda, 22nd March 2019.

- Advanced Analytical Techniques for Elemental Analysis (AAT-2019), MSU, Baroda, 28th Dec 2019.

CONFERENCE PROCEEDING

- Sudhakar P, Chakraborty D, **Patel D**, Ravi P, Sahoo S. Pre-and post-monsoon variation of uranium and associated water quality parameters in Narmada district of Gujarat. *The twentieth National Symposium on Environmental in Energy Resource Management and Climate Change*, IIT Ghandhinagar, Ghandhinagar, Gujarat, 2018.

Environmental Nanotechnology, Monitoring & Management 18 (2022) 100732

Contents lists available at ScienceDirect

Environmental Nanotechnology, Monitoring & Management

journal homepage: www.elsevier.com/locate/enmm

Bharuch District, Gujarat, India: Factor analysis and geographical distribution of water quality characteristics

Divya Patel [a], Padmaja Pamidimukkala [a,b,*], Debjani Chakraborty [b], Akhilesh Yadav [c]

[a] Department of Environmental Studies, The Maharaja Sayajirao University of Baroda, Vadodara 390002, India
[b] Department of Chemistry, The Maharaja Sayajirao University of Baroda, Vadodara 390002, India
[c] Environmental Science and Engineering Department, Indian Institute of Technology Bombay, Mumbai 400 076, India

ARTICLE INFO

Keywords:
Factor analysis
Spatial distribution
Groundwater quality
Uranium

ABSTRACT

The goal of this study was to use statistical methods to create baseline data on uranium and associated physicochemical characteristics in the Bharuch district. The district is 6,527 km2 in size and is situated at 21.7051° N, 72.9959° E. Factor analysis is a crucial tool in statistical analytical approaches for obtaining general relationship between measured varaibles. For the study, 144 samples were collected from the Bharuch district of Gujarat during the pre-monsoon (PRMNS) and post-monsoon (POMNS) seasons. A portable multi-parameter water analysis tool was used to test in-situ water quality parameters on-site. In the laboratory, the uranium concentration and the other parameters were examined. Principle component analysis was performed on the data that led to reduction of 18 parameters to 6 during PRMNS and POMNS periods. The eigenvalue-extracted factor generated 86.01 percent and 86.017 percent variation in the PRMNS and POMNS, respectively.

1. Introduction

Water quality evaluation and monitoring is one of the most important and high-priority aspects of environmental policy (Yousry and El Gammal, 2015; Love et al., 2004). Its main goal is to regulate and reduce the occurrence of pollutant-related problems, as well as to deliver water of suitable quality for diverse applications such as drinkable and irrigation water. The biological, Chemical and, Physical properties of water are used to determine its quality (Yousry and El Gammal, 2015; Sargaonkar and Deshpande, 2003; Liu et al., 2003). Natural processes such as rock types, mineral weathering rates, precipitation rates, and soil quality, as well as anthropogenic factors such as urbanization, industrialization, agricultural activities, and overexploitation of water resources, influence groundwater quality within a region. Principal component analysis is a valuable approach for determining which geogenic and anthropogenic factors are to blame for variations in groundwater physicochemical characteristics (Bodrud-Doza et al., 2018; Muangthong and Shrestha, 2015). The research area has a semi-arid environment with a variety of aquifers and groundwater quality. Spatial and temporal water quality assessment, pollutant source identification, multivariate statistical approaches for data analysis and elucidation are all useful (Zarei and Pourreza Bilondi, 2013) for efficient water quality management. In a typical water quality assessment programme, many parameters are measured at various monitoring locations over a period of time. As a result, a complicated data matrix should be evaluated to assess water quality (Gupta et al., 2005). Multivariate statistical methodologies allow for the extraction of hidden information regarding probable environmental influences on water quality from a data collection. Factor analysis tries to explain relationships between data in terms of underlying components that are not readily visible. According to literature reports, factor analysis has three stages. A correlation matrix is constructed for all variables, and factors are extracted from the correlation matrix using the correlation coefficients of the variables (Love et al., 2004; Berisha and Goessler, 2013).

Fluoride, uranium, and other inorganic pollutants of groundwater are geogenic sources, with uranium occurring in groundwater/or drinking water as a result of natural deposits, and also anthropogenic activities such as nuclear power plant emissions, coal and fuel combustion, and the usage of phosphate fertilizers (Birke et al., 2010; Kaushik et al., 2020). Uranium is considered an emerging pollutant in groundwater/drinking water across the world (Table S1). A high concentration of fluoride was also reported across India (Table S2). Fluoride is found in drinking water as a result of anthropogenic activities such as the synthesis and application of phosphate fertilisers, hydrofluoric acid

* Corresponding author at: Department of Environmental Studies, The Maharaja Sayajirao University of Baroda, Vadodara 390002, India.
E-mail address: padmaja.sudhakar-chem@msubaroda.ac.in (P. Pamidimukkala).

https://doi.org/10.1016/j.enmm.2022.100732
Received 19 June 2022; Received in revised form 12 July 2022; Accepted 24 July 2022
Available online 28 July 2022
2215-1532/

manufacture and usage, aluminium, steel, and oil production, and the burning of fluoride-rich coals. Apart from geogenic, volcanic emissions are also a source of fluoride (Singh Sankhla and Kumar, 2018). Fluoride and uranium can cause serious health hazards such as fluorosis and nephrotoxicity respectively (Sharma et al., 2019; GCWB, 2014).

In the present study, fluoride and uranium along with associated water quality parameters were analyzed in groundwaters of Bharuch district and spatial distribution of fluoride and uranium along with nitrate, phosphate, alkalinity, hardness, TDS, sulfate, chloride, etc. have been depicted. Further, factor analysis of groundwater pollutants and correlation of all parameters with each other have been studied.

2. Interpretation of study area

Bharuch is a district in Gujarat, India (Fig. 1), on the banks of Narmada River, with an average elevation of 15 m, Bharuch is located at 21.712°N 72.993°E, with Vadodara to the north, Narmada to the east, Surat to the south, and Gulf of Khambhat to the west.

The Arabian Sea has a tremendous influence on the weather in Bharuch. The summer season runs from early March through late June. The hottest months are April and May, with average high temperatures of 40 °C. The monsoon season begins later in June and lasts until the end of September, when it receives roughly 800 mm of rain. During the wet season, the average maximum temperature is 320 °C. The temperature begins to climb again in October until late November, when winter begins.

2.1. Geology, Geography, and hydrogeology of the study area

Bharuch district features a diverse landscape, as well as a diverse geology. There are four topographic units that make up the entire area (Fig. 1).

1. Hilly area with high relief
2. Piedomont zone
3. Alluvial plain
4. Coastal area

The district's geology, which includes large areas influenced by coastal salt, creates a complex hydrogeological pattern. Fig. 1 depicts a hydrogeological map. Multi–aquifer systems are created by semi-consolidated Cretaceous, hard rocks, and tertiary formations, as well as unconsolidated alluvial deposits, resulting in both unconfined and confined groundwater conditions across the area. Tertiary deposits are naturally salty and have low groundwater quality. The limestone and sandstone aquifers of the Bagh deposits contain unconfined groundwater (last cretaceous marine sediment). For occurrence and movement, groundwater is restricted to the fractures and joints in limestones and sandstones. Deccan Trap overlain the bagh layers, which are prone to release groundwater under constrained conditions (APHA, 2017).

3. Materials and methodology

3.1. Preparation in the laboratory before sample collection

The selected district was divided into 6x6 km^2 grids with the help of SySGlob Software Solutions Limited, which is an IT company, in Bengaluru, Karnataka, India to perform systematic grid sampling. All polyethylene bottles that will be used for sampling were adequately cleaned with diluted nitric acid and then washed with conductivity water before going out into the field.

3.2. Collection of samples

The samples were taken from each grid (red triangles) of the entire

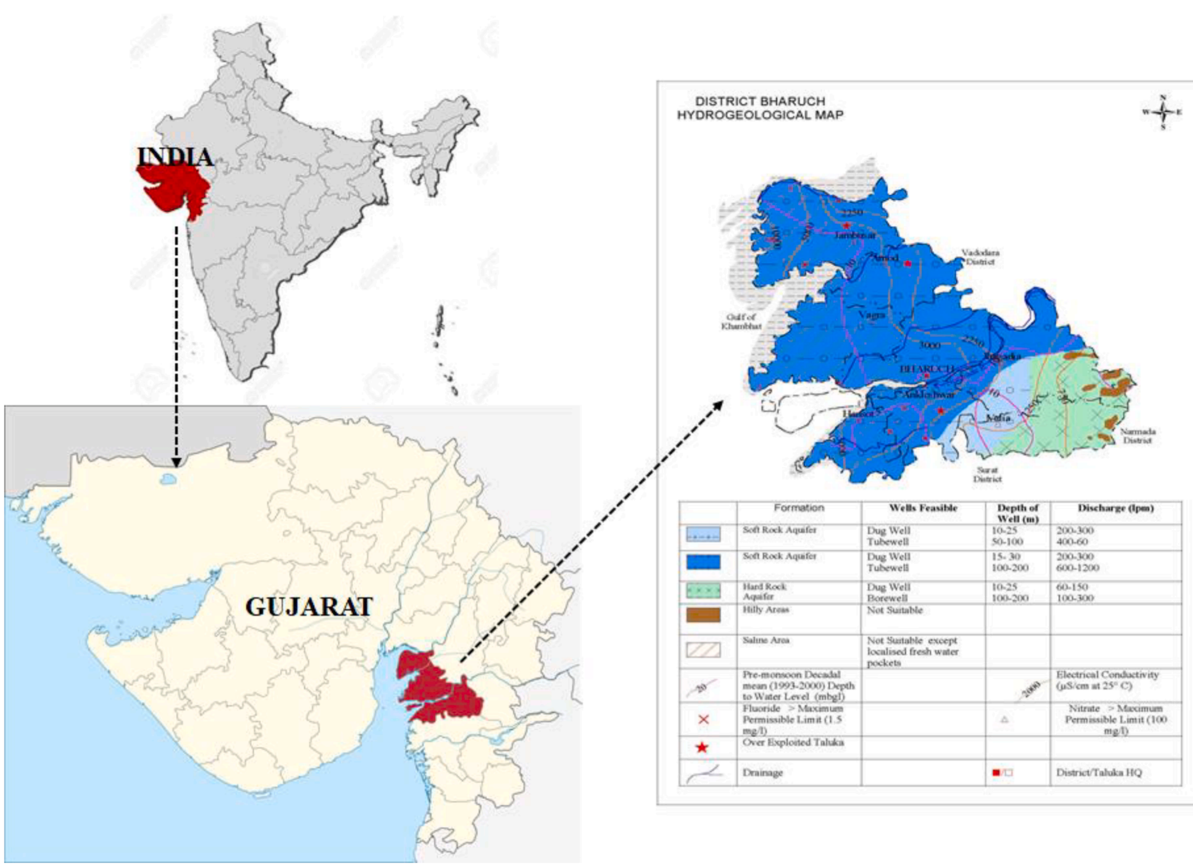

Fig. 1. Showing the location and hydrogeological map of Bharuch district (APHA, 2017).

area during PRMNS and POMNS seasons (Fig. S1a & b), using a GPS (GarminGPSmap 70 s). The collected samples were from various sources like handpumps (30 %), bore wells (28 %), water tanks (30 %), open wells (6 %), and pipelines (6 %) (Fig. S2) of varying depths, amounting to 144 samples located nearby the resident's houses and were being regularly used in the house-hold. In the case of handpumps and bore wells, the water was kept running for 5–10 min but in the case of open wells, water tanks, and pipelines water was taken directly from the source in polyethylene bottles which were properly rinsed with diluted nitric acid and then cleaned with conductivity water. The bottles were further thoroughly cleaned 2–3 times with the water sample to be collected. For uranium analysis, the samples were collected separately in another 100 mL bottle and acidified with 1–2 drops of nitric acid. Water samples were preserved by maintaining at 4 °C till further analysis.

3.3. Estimation of various physicochemical parameters

Parameters such as pH, Oxidation-Reduction Potential (ORP), Electrical Conductivity (EC), dissolved oxygen (DO), Total Dissolved Solids (TDS), salinity, and temperature were analyzed on-site during sampling with the help of Thermo Scientific- Orion Star A329 model, pH/ISE/Conductivity/RDO/DO meter. Other parameters like phosphate, nitrate, and sulfate were determined by using a UV spectrophotometer. Mohr's procedure was used to analyze the chloride ions. The titrimetric method was used to determine total alkalinity (TA). The EDTA titration method was used to measure total hardness (TH), calcium hardness (CaH), and magnesium hardness (MgH) was computed theoretically. All of the processes used in the analysis were standard methods for water testing (WHO, 2011).

3.4. Uranium estimation

For uranium estimation LED-fluorimeter LF-2 model designed and manufactured by Quantalase Enterprises Pvt. ltd, Indore, India was used. This method was based on luminescence property of uranyl ion in solution. A solution of five percent sodium pyrophosphate in distilled water was prepared, and the pH was adjusted to 7 with orthophosphoric acid. This solution was then added to the water sample in a 1:10 ratio to convert all uranium species into a single form and enhance fluorescence. To prevent the matrix effect, the uranium concentration in the sample was determined using the standard addition method. The following formula was used to compute the concentration:

$$\text{Calibration factor (CF)} = \frac{\text{Conc. of uranium in standard solution}}{\text{Fluorescence of standard} - \text{fluorescence of water}}$$

$$\text{Conc. of uranium in sample} = \text{CF X (fluorescence of sample} - \text{fluorescence of water)}$$

3.5. Estimation of fluoride

Fluoride concentration in water samples was estimated by Ion-Selective Electrode (ISE) of Orion as per the Orion application procedure and was read directly by Ion-selective electrode (Thermo Scientific Orion Star A214-pH/IES meter). Fluoride stock solution (1000 ppm) was prepared from sodium fluoride and stored in polyethylene labware, to be further used for the preparation of 1 ppm, 5 ppm, and 10 ppm standards for instrument calibration. Total ionic strength adjustment buffer-III (TISAB-III) solution contains sodium chloride (NH_4Cl), 1, 2-cyclohexanediamine-N,N,N',N'-tetraacetic acid-$C_{14}H_{22}N_2O_8{\cdot}H_2O$ (CDTA), Ammonium acetate (CH_3COONH_4), CRESOL RED ($C_{21}H_{18}O_5S$), and deionized water. The TISAB solution controls the pH and regulates the ionic strength of samples and reference solutions (WHO, 2011).

3.6. Statistical analysis

All descriptive statistics such as average, standard deviation, standard error, minimum, and maximum for the subjected parameters were estimated by using Excel software.

4. Results and discussion

4.1. Water chemistry of study area and distribution of physicochemical parameters

Sampling areas were shown in Fig. S1a & b along with latitude and longitude (Table S3). Table 1 shows the statistical results of water chemistry for PRMNS and POMNS (n = 144), as well as the box plot in Fig. 2(a & b) for PRMNS and POMNS, respectively. For the groundwater samples collected from the study region, uranium and various physicochemical parameters such as pH, EC, TDS, DO, ORP, temperature, Total hardness, Total alkalinity, and calcium, magnesium, carbonate, bicarbonate, chloride, fluoride, nitrate, sulphate, and phosphate ion concentrations were analysed. According to the findings, the groundwater was mildly alkaline, with an average pH of 7.67 and 8.12 during PRMNS and POMNS, respectively, falling within the WHO-recommended range of 6.5–8.5 (Hem, 1959). The dissolved carbonate and bicarbonate equlibria controls the pH of the groundwater, which is a highly essential indicator of groundwater quality (Antony et al., 2020).

The average TDS in groundwater samples of the study area was found to be 968.68 ppm and 1200.81 ppm in PRMNS and POMNS respectively, which are above the permissible limit of 600 ppm recommended by the WHO. The high TDS content in the PRMNS can be due to high leaching rate of pollutants and high dissolution of parental rock (Nayak et al., 2008).

The fluoride concentration varied from 0.05 to 2.07 ppm and 0.096–1.8 ppm in PRMNS and POMNS respectively. It was observed that the fluoride content of 1.38 % of samples was above the permissible limit of WHO in both seasons (PRMNS and POMNS) while the average concentration of fluoride (0.40 ppm) was below the permissible limit of WHO in both seasons. The high concentration of fluoride can be due to the local lithology of the study area (Molly Hunt and Herron, 2012).

The average concentrations of chloride (permissible limit – 1000 ppm), nitrate (permissible limit – 45 ppm, sulfate (permissible limit – 400 ppm), and phosphate were 400.44 ppm, 9.02 ppm, 84.96 ppm, and 0.12 ppm in PRMNS respectively, while during POMNS season the concentration of the same parameters were 444.8 ppm, 12.1 ppm, 116.2 ppm, 0.1 ppm respectively, which were below the permissible limit of WHO. High chloride levels in groundwater can be caused by natural and anthropogenic activities such as landfill leachates, septic tank effluents, animal feeds, industrial effluents, agricultural runoff and seawater intrusion in coastal areas (AERB, 2004).

The average concentration of uranium was below the permissible limit of WHO (30 ppb) and AERB (60 ppb) limits (Hem, 1959; Shah et al., 2021). During POMNS the concentration varied from 0.1 to 18.4 ppb while during PRMNS the concentration varied from 0.1 to 28.40 ppb.

Table 1
Showing water chemistry of study area.

Parameters	PRMNS						POMNS						BIS 2012/ (HEM, 1959) limits	
	Min	Max	Average	Median	SD	SE	Min	Max	Average	Median	SD	SE	Desirable limit	Allowable limit
pH	6.43	8.94	7.67	7.60	0.55	0.05	6.26	10.22	8.12	7.93	0.75	0.06	**6.5 – 8.5**	9.2
TDS (ppm)	81.05	8173.00	968.68	693.10	959.39	79.95	167.4	6580	1200.81	871.4	1042.86	86.90	**600**	1000
EC (µS/cm)	164.40	16690.00	2015.52	164.40	1971.52	164.29	341.4	13,960	2452.89	1779	2146.99	178.92	–	1500
Salinity (ppm)	65.45	9968.73	1034.42	65.45	1132.91	94.41	140	9327	1349.95	912.5	1387.11	115.59	–	–
ORP (mV)	−106.00	26.70	−35.42	−106.00	30.00	2.50	−139.3	30.5	−56.33	−49.25	30.41	2.53	–	–
Temp. (^0C)	21.30	36.00	30.13	30.50	2.70	0.22	18.7	31.6	26.60	27.25	2.97	0.25	–	–
DO (ppm)	1.02	9.51	4.68	4.67	2.38	0.20	1.71	11.2	5.31	4.955	2.36	0.20	–	–
F^- (ppm)	0.05	2.07	0.40	0.29	0.32	0.03	0.0966	1.98	0.49	0.3975	0.30	0.02	**1**	1.5
Cl^- (ppm)	12.00	5760.21	400.44	177.94	633.20	52.77	10.0	2689.2	444.8	226.9	549.89	45.82	**250**	1000
NO_3^- (ppm)	0.50	85.78	9.02	3.70	14.99	1.25	0.5	235.4	12.1	3.9	26.14	2.18	**45**	–
SO_4^{2-} (ppm)	2.50	507.04	84.96	52.23	94.57	7.88	8.3	1172.4	116.2	59.0	164.79	13.73	**150**	400
PO_4^{3-} (ppm)	0.10	1.35	0.12	0.10	0.11	0.01	0.1	0.6	0.1	0.1	0.05	0.00	–	–
U (ppb)	0.10	28.40	5.05	1.61	10.07	0.84	0.1	18.4	1.8	0.1	3.42	0.28	–	30
T H (ppm)	24.00	2232.00	380.33	268.00	322.27	26.86	58.0	2122.0	482.0	366.0	359.28	29.94	**300**	600
Ca^{2+} (ppm)	8.00	1056.00	141.35	104.00	126.13	223.66	8.0	1060.0	200.5	144.0	178.19	14.85	**75**	200
Mg^{2+} (ppm)	16.00	1376.00	238.98	144.00	223.66	18.64	50.0	1134.0	281.5	200.0	219.09	18.26	**50**	150
TA(ppm)	50.04	950.82	285.00	270.23	147.03	12.25	50.0	1151.0	348.5	350.3	178.76	14.90		
HCO_3^- (ppm)	50.04	950.82	282.11	250.22	146.05	12.17	10	1151.0	341.3	340.3	185.07	15.42	–	**300**

The average concentration of hardness, in terms of CaH, and MgH were above the permissible limit of WHO, which were 380.33 ppm, 141.35 ppm, and 238.98 ppm in PRM while in POM it was 482.0 ppm, 200.5 ppm, and 281.5 ppm respectively. The permissible limit of TH, Ca^{2+}, and Mg^{2+} are 600 ppm, 200 ppm, and 150 ppm respectively. The average concentration of bicarbonate was 282.11 ppm and 341.3 ppm in PRMNS and POMNS seasons respectively indicating the temporary hardness of water (Rapant et al., 2017). Calcium ion and magnesium ion are essential elements for human health maintenance and development. Calcium is very important for the development of healthy bones and teeth, as well as cardiovascular health (Hem, 1959). The high concentrations of calcium and magnesium ions in the groundwater may have a negative impact on human health. While a high intake of calcium and magnesium can cause cardiovascular disease, high magnesium can also have a laxative effect (Sengupta, 2013; Kumar et al., 2016).

4.2. *Factor analysis*

The findings of the water quality test, which included uranium concentrations for both PRMNS and POMNS seasons, were organised in a matrix with variables columns and rows for 144 samples. Statistical software was used to analyse the data statistically (SPSS version 19). The factor extraction was done using a non-confirmatory principal component analysis. To analyse the output data of the study region, correlation, total variance, scree plot, component matrix (rotated and unrotated), and factor values were employed. For both seasons, the extracted scree plots are displayed in Fig. 3(a & b). The scree plots show how the different principal components (PC)were extracted, as well as the percentage variances for each component. The Scree plots show a pronounced change of slope after the third eigenvalues for both PRMNS and POMNS seasons.

Eigenvalues indicate that the first three PC are the most significant components which represent about 70 % of the variance in water quality of the study area (39.5 % by PC1, 15.2 % by PC2, 12.6 % by PC3) with first PC contributing to 40 % during PRMNS study. On the other hand, the first two PCs are the most significant components contributing to 60 % of the variance in water quality with the first PC contributing to about 40 % during the POMNS study too.

The largest positive or negative component loadings (correlation coefficients), represent the degree of proximity between the variables and a PC. Positive loading shows that the contribution of the variables increases as the PC increases; negative loading indicates that the contribution of the variables decreases.

The eigenvalues for various factors, percentage variance, cumulative percentage variance, and component loadings (unrotated and rotated), are shown in Table 2 during PRMNS and POMNS.

In factor analysis, the eigenvalue was set to 1 as the threshold value for extracting each component, which is important for explaining the source of variance in the data. According to descriptive statistics, several water quality indicators such as TDS, EC, salinity, hardness, alkalinity, and others have a significant standard deviation. The research area is classified as semiarid. According to some previous studies, water pollution is caused by the discharge of untreated waste form industries into some water bodies, rendering the water unfit for drinking and domestic use (Gupta, 2016), Other natural sources of water pollution include acid rain, weathering of parents rock, and other natural disasters (Dilbeck, 2018), Municipal sewage, untreated man-made activities on unlined surfaces, excessive fertiliser use in agriculture, and industrial effluent all contribute to greater ion concentrations in groundwater aquifers (APHA, 2017). Table 3 (for both seasons) shows the principal components (Varimax rotation and after rotation), as well as the eigenvalues and variance percentage. The PCA was created using the correlation coefficient between the many parameters that were tracked using varimax rotation (Magnello and Kempf-Leonard, 2005). A factor analysis was performed on 20 parameters collected from 144 sampling locations. Table 2 shows that cumulative extraction of squared loadings

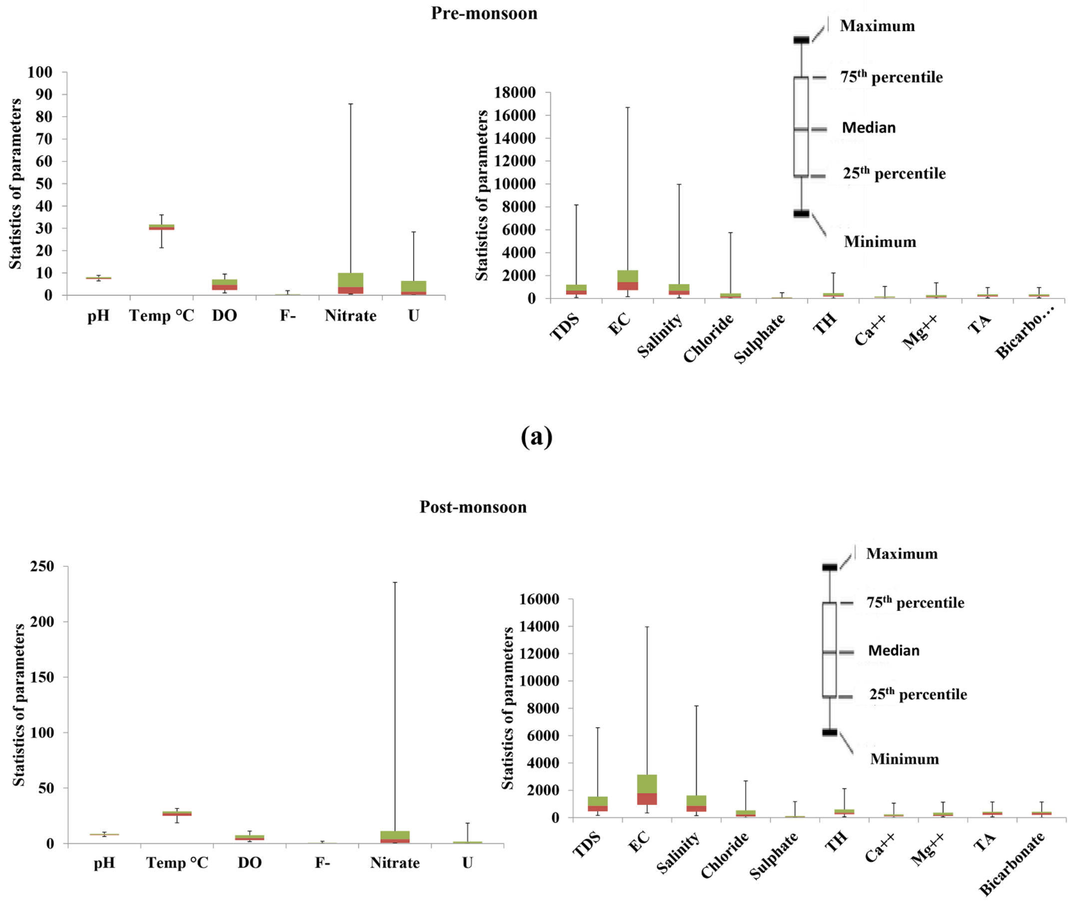

Fig. 2. The concentration of physicochemical parameters PRMNS and POMNS of data is shown in a box-whisker plot (a & b respectively). The median value is represented by the centre line within the box. The 25th percentile is at the lower end and the 75th percentile at the upper end of the box.

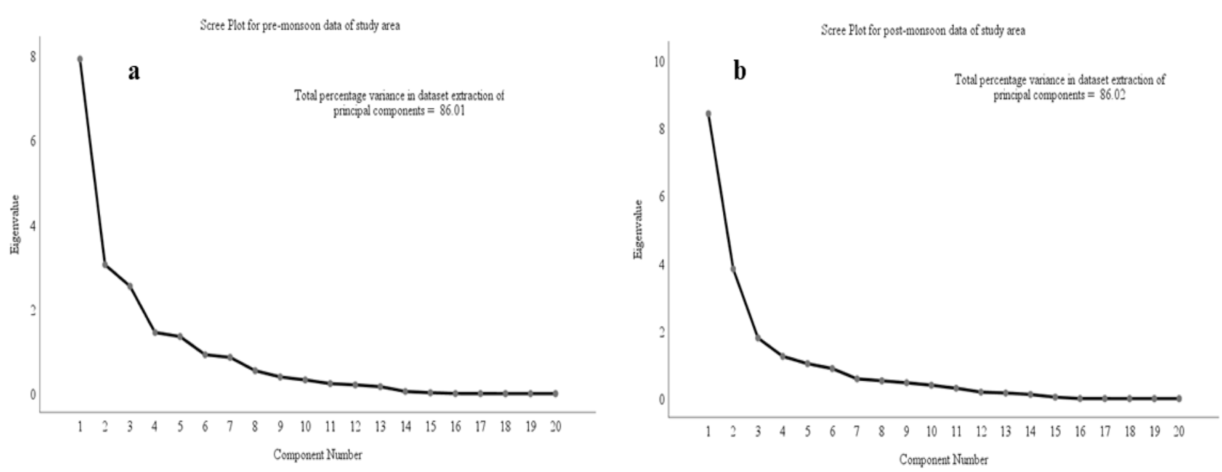

Fig. 3. In a scree plot, data of water quality is plotted (a. PRMNS, b. POMNS).

is 86.01 percent in the POMNS and 86.02 percent in the PRMNS.

Factor 1.

Factor 1 (Table 3) is heavily loaded (factor score > 0.50), with main parameters such as TDS (0.918), EC(0.919) salinity (0.909), chloride (0.54), nitrate (0.537), sulphate (0.772), uranium (0.682), total hardness (0.96), calcium hardness (0.772), and magnesium hardness (0.856) accounting for 32.701 percent in PRM, and TDS (0.918 The first factor, salinity, chloride, hardness, and bicarbonates, accounted for 32.701 percent in PRMNS and 33.413 percent in POMNS, respectively. Rapid development and over-exploitation of groundwater may be the cause, according to the current analysis, due to a rise in salt concentration or excessive fertilizer use. The same conclusions were reported by many researchers and some government statistics (APHA, 2017; Gupta, 2016).

Factor 2.

In PRMNS season the second factor (Table 3) was positively loaded only with pH (0.508), DO (0.635) while in POMNS season it was

Table 2
For the study area, values for several factor analysis parameters were extracted.

Component	Total Variance Explained					
	Pre-monsoon					
	Extraction Sums of Squared Loadings			Rotation Sums of Squared Loadings		
	Total(Initial Eigenvalue)	% of Variance	Cumulative %	Total	% of Variance	Cumulative %
1	7.906	39.532	39.532	6.540	32.701	32.701
2	3.047	15.234	54.766	2.886	14.429	47.130
3	2.537	12.687	67.453	2.709	13.545	60.675
4	1.443	7.217	74.670	2.117	10.586	71.261
5	1.349	6.744	81.414	1.916	9.578	80.839
6	0.919	4.596	86.010	1.034	5.171	86.010
	Post-monsoon					
1	8.415	42.076	42.076	6.683	33.413	33.413
2	3.830	19.151	61.228	3.075	15.377	48.789
3	1.792	8.961	70.188	2.560	12.798	61.587
4	1.247	6.235	76.423	2.375	11.875	73.462
5	1.033	5.163	81.586	1.476	7.379	80.841
6	0.886	4.431	86.017	1.035	5.176	86.017
Extraction Method: Principal Component Analysis(PCA)						

Table 3
Component matrix for Principal Component analysis.

Factor (6 components extracted)												
Variables	PRMNS						POMNS					
	1	2	3	4	5	6	1	2	3	4	5	6
pH	−0.492	**0.508**	**0.517**	0.316	−0.057	0.055	−0.520	**0.734**	0.232	−0.179	−0.176	0.020
TDS	**0.918**	0.249	0.188	−0.006	−0.161	0.062	**0.879**	0.403	0.010	−0.100	0.083	0.069
EC	**0.919**	0.237	0.198	0.004	−0.168	0.062	**0.880**	0.403	0.014	−0.099	0.079	0.063
ORP	**0.476**	−0.544	−0.431	−0.405	0.137	−0.096	**0.517**	−0.732	−0.238	0.176	0.173	−0.021
Temp.	−0.319	0.383	0.192	0.249	**0.542**	0.026	0.343	−0.547	0.197	0.191	**0.499**	−0.177
Salinity	**0.909**	0.260	0.196	−0.012	−0.179	0.068	**0.823**	0.349	0.161	−0.183	0.129	0.114
DO	−0.328	**0.635**	0.133	0.369	−0.038	−0.080	−0.392	**0.640**	−0.203	−0.179	−0.186	0.029
F^-	0.300	−0.519	0.420	0.151	−0.439	−0.106	0.272	−0.127	**0.682**	−0.316	0.261	0.193
Cl^-	**0.854**	0.393	0.171	−0.089	−0.170	0.078	**0.766**	**0.475**	−0.115	−0.132	0.220	0.102
NO_3^-	**0.537**	−0.114	−0.046	0.326	0.381	−0.124	**0.726**	0.154	0.016	0.162	−0.192	−0.372
SO_4^{2-}	**0.747**	−0.022	0.161	0.194	−0.278	−0.055	**0.785**	0.212	0.205	−0.149	0.168	−0.046
PO_4^{3-}	−0.020	−0.190	0.283	−0.154	0.213	**0.862**	−0.046	0.161	0.083	**0.670**	−0.019	**0.689**
U	**0.682**	−0.049	−0.075	0.206	**0.498**	−0.144	**0.623**	0.133	0.163	0.138	−0.362	−0.082
Total hardness	**0.896**	0.300	−0.119	−0.097	0.199	−0.007	**0.842**	0.263	−0.338	0.165	−0.004	−0.024
Calcium hardness	**0.772**	0.296	−0.215	−0.337	0.068	−0.010	**0.802**	0.085	−0.298	0.292	−0.088	−0.179
Magnesium hardness	**0.856**	0.266	−0.050	0.050	0.248	−0.004	**0.728**	0.363	−0.311	0.033	0.066	0.106
Bicarbonate	**0.474**	−0.701	0.142	0.417	0.061	0.067	**0.680**	−0.372	0.458	0.048	−0.362	0.020
Carbonate	−0.078	−0.133	**0.855**	−0.387	0.213	−0.202	−0.448	**0.630**	0.357	0.391	0.194	−0.243
Total Alkalinity	**0.463**	−0.710	0.227	0.375	0.082	0.046	**0.663**	−0.326	**0.507**	0.086	−0.356	−0.002
Phenolphthalein alkalinity	−0.078	−0.133	**0.855**	−0.387	0.213	−0.202	−0.448	**0.630**	0.357	0.391	0.194	−0.243

significant scores are represented in bold.

positively loaded with pH (0.734), DO (0.640) along with Chloride (0.475), Carbonate (0.630) and Phenolphthalein alkalinity (0.663).

Factor 3.

The third factor was extracted with 12.68 % and8.961 % of variance during PRMNS and POMNS respectively. In the third factor, rotation variance was 13.54 % and 12.79 % during PRMNS and POMNS respectively. In the PRMNS third factor was positively loaded with pH, carbonate, and phenolphthalein alkalinity to a significant extent, while during POMNS it was positively loaded with only fluoride and total alkalinity to a significant extent.

Factor 4.

Factor 4, exhibited 7.21 % and 10.58 % of variance in PRMNS and POMNS seasons respectively. There was no significant loading of any parameters in factor 4 in PRMNS while in POMNS factor 4 was positively significantly loaded with phosphate (0.670).

Factor 5.

Factor 5 extracted 6.74 % and 9.57 % of variance in PRMNS and POMNS seasons respectively. In PRMNS factor 5 was significantly loaded with uranium (0.498) while in POMNS season factor 5 was loaded with temperature (0.499).

Factor 6.

Factor 6 was only significantly loaded with phosphate in both seasons i.e. 0.862 and 0.689 in PRMNS and POMNS respectively.

4.3. Correlation study

Correlation analysis of U and fluoride with other physicochemical parameters of water was done using the Karl Pearson correlation matrix based on the value of the correlation coefficient 'R' for both PRMNS and POMNS seasons to understand the distribution of uranium and fluoride and mobility using MS excel 2007.

The correlation coefficient between x and y (denoted by symbol R) was determined using the following Eq. for a set of n pairs of observations on two variables x and y (Anita Erőssa et al., 2018).

$$R = \frac{\text{cov}(x, y)}{\sigma x \sigma y} = \frac{\frac{\sum xy}{n} - \left(\frac{\sum x}{n}\right)\left(\frac{\sum y}{n}\right)}{\sigma x \sigma y}$$

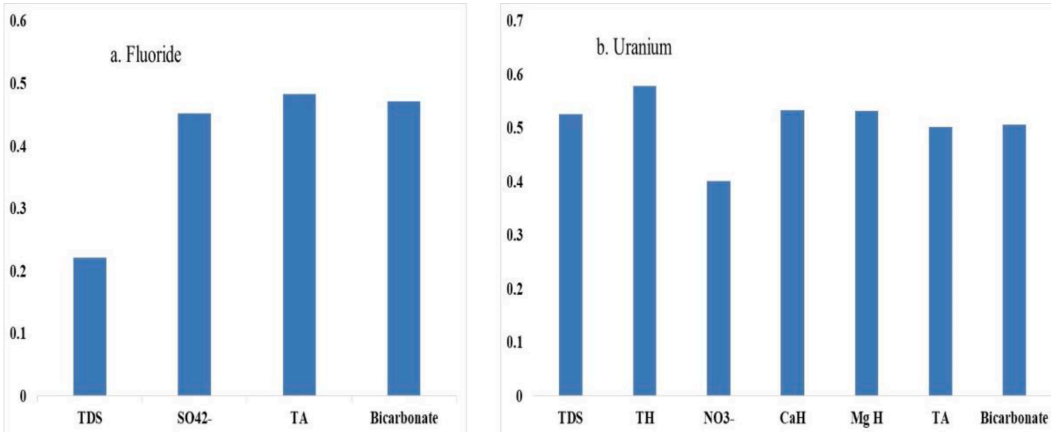

Fig. 4. Fluoride (a) and uranium (b) substantial correlation coefficients with several physicochemical parameters of groundwater samples in Bharuch district.

where σx and σy are the standard deviations of x and y respectively and cov (x,y) denotes the covariance of x and y.

The Karl Pearson correlation matrices for selected variables were prepared for groundwater of the Bharuch district (Fig. 4a & b). The hydro-geochemical behaviour of uranium is influenced by a variety of groundwater quality characteristics, including alkalinity, pH, and chemical composition, including nitrate, sulphate, hardness bicarbonate etc. (Camacho et al., 2010) and hence is complex. The possibility that groundwater samples with high TDS contain various ionic species that might interact with uranium in groundwater could explain the positive correlation of uranium content with TDS and EC during PRMNS and POMNS. It was also observed that uranium has a positive correlation with alkalinity and bicarbonate, suggesting the possibility of formation of soluble uranyl carbonate/bicarbonate complexes such as $UO_2(CO_3)_2^{2-}$ in groundwater that does not adsorb to minerals and metal oxides present in the soil (Coyte et al., 2018). Hence, alkalinity and bicarbonate play a significant role in regulating the uranium content in groundwater (GCWB, 2014; katsoyiannis et al., 2007; Adimalla, 2020). Further, the positive correlation of nitrate with uranium confirmed the possible mobilization of naturally occurring uranium and resultant contamination of groundwater.

The correlation coefficient of fluoride with bicarbonate (0.47) and with TA (0.48) was positive. The alkaline groundwater environment with high bicarbonate and TA contents was responsible for dissolution of fluoride in groundwater (Adimalla, 2020). Fluoride was weak positively correlated with TDS (0.22) and positively correlated with sulfate (0.45).

5. Conclusion

This study examines the quality of water samples obtained in the Bharuch district, and it is the first of its type to report on uranium concentrations in groundwater of Bharuch. The hydrogeology of the studied area, weathering, and leaching of parental rocks and industries all have a significant impact on groundwater composition. The average uranium and fluoride levels in the research area were determined to be within WHO acceptable limits, indicating that neither pose a health risk. The use of principal component analysis on the chemical composition of groundwater, eliminated the primary contaminants induced by anthropogenic activities for all parameters. The first factor has a positive link with salinity, TDS, chloride, hardness, bicarbonates, alkalinity, nitrate, and sulphate, indicating that it could occur as a result of an increase in salt concentration, excess fertilizers, industrialization, and overexploitation of groundwater. The first component also had a positive link with uranium, indicating that it could be attributable to parental rock weathering and groundwater over-exploitation. Overall, the samples are found to have a low concentration of the investigated parameters. However, it is necessary to monitor these sources on a regular basis to ensure the water's potability status, because if the concentration of these parameters continues to rise, it may affect the health of the inhabitants.

CRediT authorship contribution statement

Divya Patel: Data curation, Formal analysis, Methodology, Writing – original draft. **P. Padmaja Sudhakar:** Conceptualization, Funding acquisition, Investigation, Methodology, Project administration, Resources, Supervision, Validation, Visualization. **Debjani Chakraborty:** Investigation, Methodology, Project administration, Supervision, Validation, Visualization. **Akhilesh Yadav:** .

Declaration of Competing Interest

The authors declare that they have no known competing financial interests or personal relationships that could have appeared to influence the work reported in this paper.

Data availability

Data will be made available on request.

Acknowledgments

This study was funded by Board of Research in Nuclear Sciences (BRNS), DAE sanction number 36(4)/14-77-2014/BRNS/10084 under NUP. The authors would also like to acknowledge Chemistry Department, The Maharaja Sayajirao University of Baroda for laboratory facilities. The authors would like to acknowledge SySGlob Software Solutions Limited, Bengaluru, Karnataka, India for the sampling grids. Along with these authors also would like to acknowledge Sulsa travels, Vadodara for help in sample collection.

Appendix A. Supplementary data

Supplementary data to this article can be found online at https://doi.org/10.1016/j.enmm.2022.100732.

References

Adimalla, N., 2020. Assessment And Mechanism Of Fluoride Enrichment In Groundwater From The Hard Rock Terrain: A Multivariate Statistical Approach. Geochem. Int. 58, 456–471.

AERB, 2004. Drinking Water Specifications In India. Department Of Atomic Energy, In.

Anita Erőssa, K.C., Izsákb, B., Varghab, Márta, Horváthc, Ákos, Pándicsb, Tamás, 2018. Uranium In Groundwater – The Importance Of Hydraulic Regime And Groundwater Flow System's Understanding. J. Environ. Radioact. 195, 90–96.

Antony, S., Dev, V.V., Kaliraj, S., Ambili, M.S., Krishnan, K.A., 2020. Seasonal Variability Of Groundwater Quality In Coastal Aquifers Of Kavaratti Island, Lakshadweep Archipelago, India. Groundwater Sustain. Dev. 11, 100377.

APHA, 2017. Standard Methods For The Examination Of Water And Waste Water, In, American Public Health Association, American Water Works Assocition And Water Environment Federation, Washington, DC.

Berisha, F., Goessler, W., 2013. Uranium In Kosovo's Drinking Water. Chemosphere 93, 2165–2170.

Birke, M., Rauch, U., Harazim, B., Lorenz, H., Glatte, W., 2010. Major And Trace Elements In German Bottled Water, Their Regional Distribution, And Accordance With National And International Standards. J. Geochem. Explor. 107, 245–271.

Bodrud-Doza, M., Bhuiyan, M., Didar, S.M., Rahman, M., Haque, M., Fatema, K., Ahmed, N., Rakib, M., Rahman, M., 2018. Hydrogeochemical Investigation Of Groundwater In Dhaka City Of Bangladesh Using Gis And Multivariate Statistical Techniques. Groundwater Sustain. Dev. 8.

Camacho, A., Devesa, R., Valles, I., Serrano, I., Soler, J., Blazquez, S., Ortega, X., Matia, L., 2010. Distribution Of Uranium Isotopes In Surface Water Of The Llobregat River Basin (Northeast Spain). J. Environ. Radioact. 101, 1048–1054.

Coyte, R.M., Jain, R.C., Srivastava, S.K., Sharma, K.C., Khalil, A., Ma, L., Vengosh, A., 2018. Large-Scale Uranium Contamination Of Groundwater Resources In India. Environ. Sci. Technol. Lett. 5, 341–347.

Dilbeck, K.E., 2018. Factor Analysis: Varimax Rotation, Sage Publications, Inc.

GCWB, 2014. Groundwater Brochure, Bharuch District, In: Technical Report Series, Government Of India, Ministry Of Water Resources, Central Ground Water Board West Central Region, Ahmedabad, Ahmedabad.

Gupta, A.K., Gupta, S.K., Patil, R.S., 2005. Statistical Analyses Of Coastal Water Quality For A Port And Harbour Region In India. Environ. Monitor. Assess. 102, 179–200.

Gupta, A., 2016. Water Pollution-Sources, Effects And Control, Pointer Publishers Jaipur.

Hem, J.D., 1959. Study And Interpretation Of The Chemical Characteristics Of Natural Water.

Katsoyiannis, I.A., Hug, S.J., Ammann, A., Zikoudi, A., Hatziliontos, C., 2007. Arsenic Speciation And Uranium Concentrations In Drinking Water Supply Wells In Northern Greece: Correlations With Redox Indicative Parameters And Implications For Groundwater Treatment. Sci. Total Environ. 383, 128–140.

Kaushik, V., Kumar, S., Singh Sankhla, M., Kumar, R., 2020. Fluoride Pollution In Drinking Water And Its Adverse Effect On Humans & Animals. Seybold Rep. 15, 1035–1048.

Kumar, S., Amaresh, D., Chinchmaltpure, A., Cssri, I., 2016. Evaluation Of Underground Water Quality Of Bara Tract Of Bharuch District (Gujarat) 2923–2925.

Liu, C.W., Lin, K.H., Kuo, Y.M., 2003. Application Of Factor Analysis In The Assessment Of Groundwater Quality In A Blackfoot Disease Area In Taiwan. Sci. Total Environ. 313, 77–89.

Love, D., Hallbauer, D., Amos, A., Hranova, R., 2004. Factor Analysis As A Tool In Groundwater Quality Management: Two Southern African Case Studies. Phys. Chem. Earth, Parts A/B/C 29, 1135–1143.

Magnello, M.E., 2005. Pearson, Karl. In: Kempf-Leonard, K. (Ed.), Encyclopedia Of Social Measurement. Elsevier, New York, pp. 31–39.

Hunt, Molly, Herron, E., Green, A.L., 2012. Chlorides In Fresh Water, Uri Watershed Watch.

Muangthong, S., Shrestha, S., 2015. Assessment Of Surface Water Quality Using Multivariate Statistical Techniques: Case Study Of The Nampong River And Songkhram River, Thailand. Environ. Monit. Assess. 187, 548.

Nayak, A.K., Chinchmalatpure, A.R., Rao, G.G., Jha, S.K., Khandelwal, M.K., 2008. An Assessment Of Fluoride In The Coastal Aquifer Of The Bara Tract In Bharuch District, Gujarat (India). Environ. Monitor. Assess. 158, 315.

Rapant, S., Cvečková, V., Fajčíková, K., Sedláková, D., Stehlíková, B., 2017. Impact Of Calcium And Magnesium In Groundwater And Drinking Water On The Health Of Inhabitants Of The Slovak Republic. Int. J. Environ. Res. Public Health 14, 278.

Sargaonkar, A., Deshpande, V., 2003. Development Of An Overall Index Of Pollution For Surface Water Based On A General Classification Scheme In Indian Context. Environ. Monitor. Assess. 89, 43–67.

Sengupta, P., 2013. Potential Health Impacts Of Hard Water. Int. J. Prev. Med. 4, 866–875.

Shah, M., Patel, H., Viramgama, P., Varanava, D., Maheshwari, D., 2021. Characterization And Assessment Of Groundwater Aquifers From Bakreshwar And Tantloi Geothermal Fields For Its Industrial Applications. Groundwater Sustainable Dev. 12, 100535.

Sharma, T., Sharma, A., Kaur, I., Mahajan, R.K., Litoria, P.K., Sahoo, S.K., Bajwa, B.S., 2019. Uranium Distribution In Groundwater And Assessment Of Age Dependent Radiation Dose In Amritsar, Gurdaspur And Pathankot Districts Of Punjab, India. Chemosphere 219, 607–616.

Singh Sankhla, M., Kumar, R., 2018. Fluoride Contamination Of Water In India And Its Impact On. Public Health 3, 10–15.

WHO, 2011. Guideline For Drinking Water Quality, In: W.H. Organization (Ed.), World Health Organization, Geneva, Switzerland.

Yousry, M., El Gammal, H., 2015. Factor Analysis As A Tool To Identify Water Quality Index Parameters Along The Nile River, Egypt.

Zarei, H., Pourreza Bilondi, M., 2013. Factor Analysis Of Chemical Composition In The Karoon River Basin, Southwest Of Iran, Applied Water. Science 3, 753–761.

Environmental Science and Pollution Research
https://doi.org/10.1007/s11356-023-25711-4

ENVIRONMENTAL IMPACTS AND CONSEQUENCES OF URBAN SPRAWL

Check for updates

Gamma radiation dose rate distribution in the Anand, Bharuch, Vadodara, and Narmada districts of Gujarat, India

Divya Patel[1] · Manoj Kumar Jindal[2,3] · Padmaja Sudhakar Pamidimukkala[1,4] · Debjani Chakraborty[4]

Received: 24 September 2022 / Accepted: 31 January 2023

Abstract
Radiation is present everywhere in the earth, and human beings are continuously exposed to gamma radiation. The health consequences of environmental radiation exposure are a serious societal issue. The purpose of this study was to analyse outdoor radiation in four districts of Gujarat, India: Anand, Bharuch, Narmada, and Vadodara during summer and winter seasons. This study illustrated the influence of lithology of areas on gamma radiation dose values. Summer and winter seasons are the primary factors that alter the causes directly or indirectly; therefore, the influence of season fluctuation on radiation dose rate was investigated. The annual dose rate and mean gamma radiation dose rate values from four districts were found to be greater than the global population weight average value. The mean value of gamma radiation dose rate from 439 locations in the summer and winter seasons was 136.23 nSv/h and 141.58 nSv/h, respectively. According to a paired differences sample study, the significance value between outdoor gamma dose rate in summer and winter seasons was 0.05 indicating that seasons have a significant impact on gamma radiation dose rate. The impact of various types of lithology on gamma radiation dose was studied in all 439 places, and the statistical analysis revealed that there was no significant association between lithology and gamma radiation dose rate in the summer season, but a relationship between lithology and gamma dose rate was observed in the winter season.

Keywords Gamma radiation · Lithology · Outdoor radiation · Seasonal variation

Introduction

Gamma radiation is abundant everywhere on the planet, and it is considerably more prevalent inside homes than outdoors. Outdoor gamma dose rate is more important in understanding the radiation distribution scenario of a place. Natural environmental radioactivity and corresponding background radiation depends on the geological and geographical conditions. This radiation comes from the soils, rocks, and lithosphere of the surrounded areas (Almayahi et al. 2012). People are constantly exposed to background radiation from both natural and artificial sources. Naturally occurring radioactive elements are found in almost all compartments of the environment (Cooper 2005). The common long-lived radioactive elements such as thorium and uranium are slowly producing other radioactive elements, such as Ra, which further undergo radioactive decay. Most building materials made from rocks, soil, and other natural sources consist significant levels of naturally occurring radioactive nuclides (Yu et al. 1992; Jindal et al. 2018a). Natural radiation existed since the earth's creation, and is impossible to avoid (Gusain et al. 2012). The soil and rocks rich with U^{238} lead to high release of radon gas, which is considered the largest source of radiation exposure (UNSCEAR 2000). Since natural radiation is the main source of the population's external exposure, it is crucial to assess the gamma radiation dose rate coming from these sources. Numerous national and international studies have been published to

Responsible Editor: Georg Steinhauser

✉ Padmaja Sudhakar Pamidimukkala
padmaja.sudhakar-chem@msubaroda.ac.in

Manoj Kumar Jindal
manojjindal1989@gmail.com

1 Department of Environmental Studies, The Maharaja Sayajirao University of Baroda, Vadodara, India

2 Indian Institute of Technology, Bhilai, India

3 Present Address: Divecha Centre for Climate Change, Indian Institute of Science, Bangalore, India

4 Department of Chemistry, The Maharaja Sayajirao University of Baroda, Vadodara, India

Published online: 18 February 2023

estimate the levels of background gamma radiation on the earth and determine the population's exposure to radiation (Gusain et al. 2012; Harikrishnan et al. 2018; Jindal et al. 2018a, 2021; Jindal and Sar 2020b; Guarino et al. 2022). Gamma radiation measurements and its distribution are crucial for identifying any variations in activity over time based on radioactive emission. Gamma rays can enter into the body and destroy cells, as well as pose a stochastic health risk depending on the likelihood of causing genetic damage and cancer. Radiation may injure cells or pass through them without causing any harm as the human body is capable to repair the cells through self-repair mechanism. However, there is certain possibility of permanent damage to the cells in case of high dose or long-time span exposure (Jindal and Sar 2020a; Jindal et al. 2021).

The current study aims to quantify the natural gamma radiation dose rate in Gujarat State of India from a few districts, namely Anand, Bharuch, Narmada, and Vadodara district so as to create a baseline database on the levels of gamma radiation and the concentration of natural radionuclides in the vicinity of the research locations. So, such research would be useful in determining the radioactive influence on the surroundings and the local population. This study also includes investigation of the spatial distribution, geological, and seasonal impact on gamma radiation dose rate. This study will also give ideas for policymakers regarding control and prevention of gamma radiation exposure for these regions.

Study area

Geology and geography of study area

he Indian peninsula's western shore is where Gujarat State is located. The study areas are shown in Fig. 1 which includes Anand, Vadodara, Narmada, and Bharuch districts of Gujarat. The Anand District is located between latitudes of 22° 06′ and 22° 43′ in the north and longitudes of 72° 20′ and 73° 12′ in the east. The population and covered area of the district are 2.09 million and 2941 km^2 (Anand District Administration 2022). The Mahisagar district borders Anand district on the north, the Gulf of Cambay (Khambhat) on the south, the Panchmahals on the east, Vadodara district on the south-east, and Kheda district on the west. The area's diverse lithology, structure, and denudational as well as depositional processes have combined to produce the current physiographic configuration. According to geomorphology, the region can be largely divided into three types: piedmont plain, alluvial plain, and coastal plains, which is known as Bhag (Yadav 2013). The area of the Vadodara District is 7546 km^2 where the total population is 4.17 million (Nandkeolyar and Sandhya Kiran 2019). The Panchmahal district to the north, the Anand and Kheda districts to the west, the Bharuch and Narmada districts to the south, and the Chhota Udaipur district to the east, all encircle the district. The district is traversed by the Mahi River. The geology of the Vadodara district is notable for its complete lack of Palaeozoic rocks and the development of just the highest Mesozoic rocks. The rocks in the Vadodara district range in age from Proterozoic to recent (Gupte 2012). Vadodara is to the north, Surat is to the south, the Gulf of Khambhat is to the east, and Bharuch is situated at 21.712°N 72.993°E. Both the geology and the terrain are diverse in the Bharuch district. The entire region is made up of four different topographic units, including a mountainous area with high relief, a piedmont zone, an alluvial plain, and a coastline area. A complex hydrogeological pattern is produced by the district's geology, which includes significant coastal salt effect in certain regions. Semi-consolidated Cretaceous, hard rock, and tertiary formations, as well as unconsolidated alluvial deposits, produce multi-aquifer systems in throughout the region (CGWB 2014; Patel et al. 2022).

Similarly, Bharuch, the landscape of the Narmada district is diverse which is situated at 21.8757° N, 73.5594° E. Bharuch and Narmada districts covered the area of 5246 and 2755 km^2, respectively. Population of Bharuch and Narmada districts are 15.5 and 0.59 million, respectively (Bharuch District Administration 2022; Narmada District Administration 2022). Narmada district can be divided into four topographic units, including drainage, the mountainous area with high relief, the Piedmont zone, and alluvial plain, according to the study reported by Central Groundwater Board. Basaltic rocks from the Cretaceous dominate the landscape, with no notable minerals. There is a small patch of exposed Mesozoic formations in Tilakwada Tehsil (CGWB 2014). In study area, ten types of geology and lithology of the study locations are grouped which are shown in Table 1.

Materials and method

Selection of measurement sites

Environmental gamma radiation dose rates were measured from a total of 439 sampling locations in Anand, Vadodara, Bharuch, and Narmada districts during summer and winter seasons. Based on feasibility and systematic approach, sampling areas were divided into 6 × 6 km^2 grids which are shown in Fig. 2. Gamma radiation dose was measured from each grid.

Quantitative and qualitative assessment

This study involves both quantity and quality approaches. For quantitative assessment, the study carried out in total of 439 locations involving 82, 125, 144, and 88 locations

Fig. 1 Map of study locations. **a** Aerial view of locations. **b** Districts geographical view

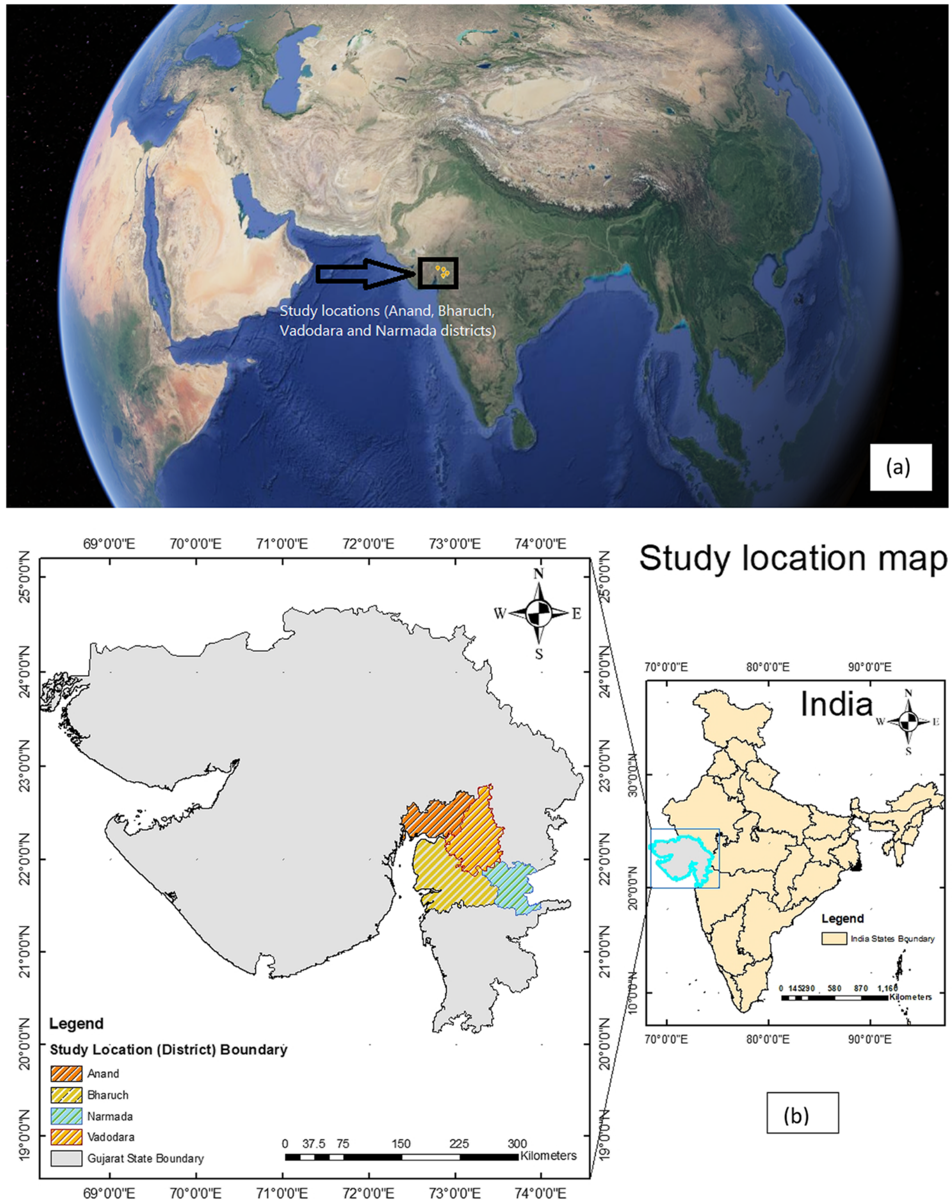

Table 1 Geology and lithology groups of study locations

Types	Lithology
1	Alluvium, blown sand, miliolite sand
2	Alluvium, blown sand, miliolite sand, shale, marls and sandstone, limestone, gypsiferous pyritous
3	Alluvium, blown sand, miliolite sand, basalts (Deccan traps)
4	Alluvium, blown sand, miliolite sand, shale, marls and sandstone, limestone, gypsiferous pyritous and carbonaceous shale
5	Alluvium, blown sand, miliolitic sand, Basalt andesite and trachytic flows
6	Alluvium, blown sand, miliolitic sand, Basalt andesite and trachytic flows, Phyllites with mangeniferous horizon, mica-shale
7	Basalts (Deccan traps)
8	Limestones and Sandstones (Bagh group) and Basalt (Deccan traps)
9	Limestones and Sandstones (Bagh group) and Quaternary alluvium
10	Shale, marls and sandstone, limestone, gypsiferous pyritous and carbonaceous shale, Basalt andesite and trachytic flows

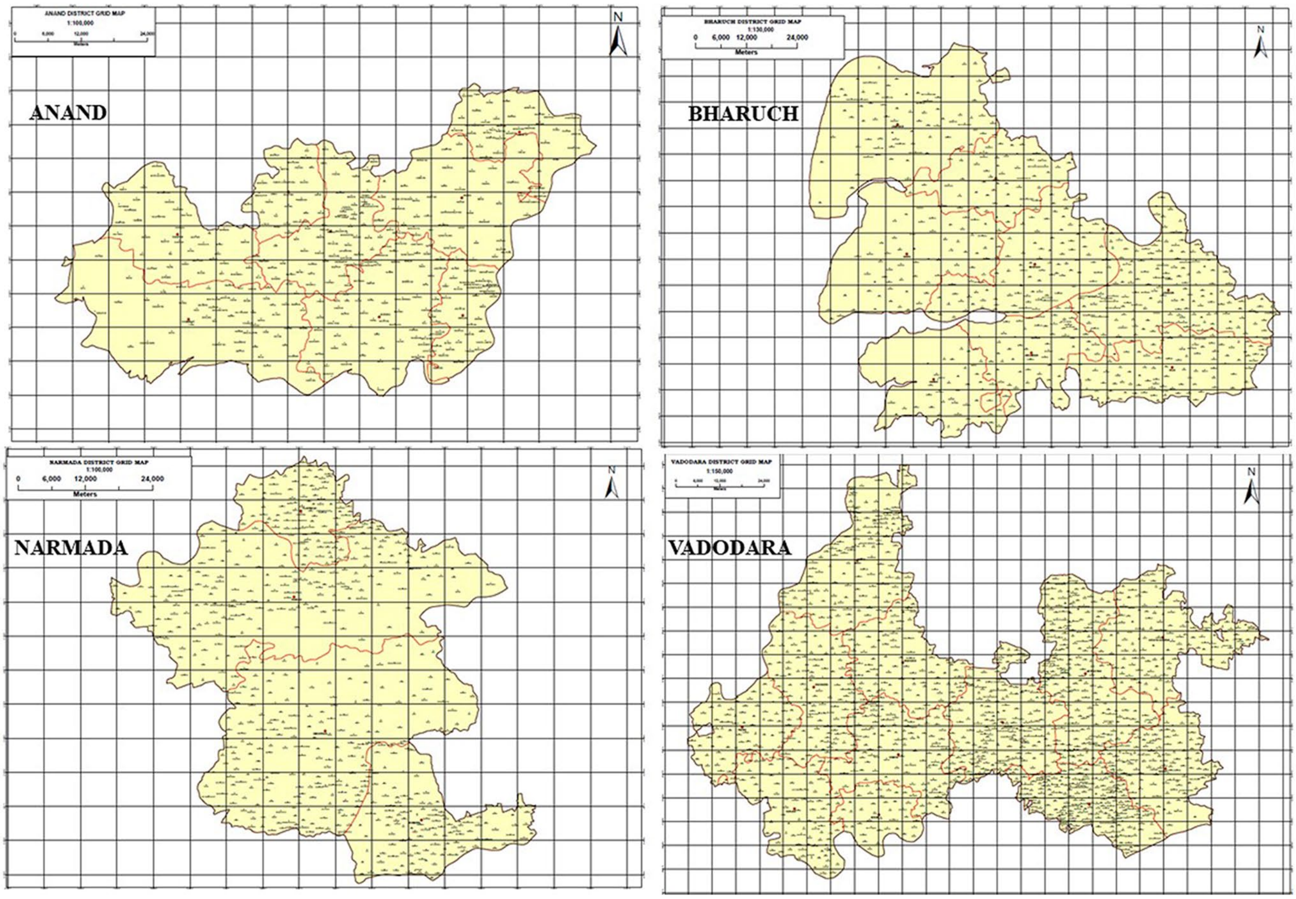

Fig. 2 Depicting grid maps of sampling locations

from Anand, Vadodara, Bharuch, and Narmada districts, respectively. All measurements were performed in summer and winter seasons. For qualitative approach, the gamma radiation dose rate from each place was measured three times to minimise the error and deviation. The constant reading with particular equipment's error has been taken for consideration.

Measurement of gamma radiation

Gamma-Scout device (Germany made) was used to quantify the dose rates of gamma radiation. The device is based on Geiger-Muller technique and it is capable to detect gamma radiation as well as alpha and beta radiation. It measures both cosmic and terrestrial radiation. Value of gamma radiation dose rate was recorded in nSv/h. For the measurement, the device was placed at 1 m above the ground. The detection range of gamma radiation dose rate measurement is 0.1 to 1000 μSv/h. The latitude and longitude of the study locations were detected using a GPS (GPS map 70 s) coordinated device.

Annual effective dose (AED)

Using the relative gamma radiation dose rates, the AED values from the study locations were determined. AED is used to analyse the biological consequences of radiation on people (NRC 2006; Jindal et al. 2018b). AED was calculated using Eq. (1) (UNSCEAR 2000):

$$\text{AED} = D \times \text{Conversion coefficient} \times T \times \text{Occupancy factor} \quad (1)$$

where D = measured gamma radiation dose rate (nSv/h), T = time conversion factor (8760 h/year). UNSCEAR (2000) reported dose conversion coefficient for an adult to be 0.7, and a higher conversion coefficient of about 0.8 and 0.9 for children and infants, respectively. The value of the occupancy factor reported by UNSCEAR for outdoor was 0.2.

Statistical analysis

The analysis of information about seasonal variability and the effects of lithology and geology as well as climatic conditions on the gamma radiation dose rate were performed using the Statistical Package for the Social Sciences (SPSS) version 23. In this study, the effect of season on the gamma radiation dose rate in the study region was estimated using the paired *t*-test, paired sample test, correlation, box plot, control chart, min, max, median, standard deviation, range, skewness, and kurtosis.

Results and discussion

Gamma radiation

The examination of outdoor gamma dose rates in four districts of Gujarat, namely Anand, Bharuch, Vadodara, and Narmada has been performed in this study. According to UNSCEAR (2000), the indoor/outdoor gamma dose rate ratio is 1.4. Very few studies were reported on the seasonal change of outdoor gamma radiation levels during last few decades (Al-Ghorabie 2005; Negi et al. 2009; Mrdakovic et al. 2012; Dhawal et al. 2013; Karunakara et al. 2014; Jindal et al. 2021). Even after these published studies, estimating the outdoor gamma radiation dose rate in seasons based on a single season remains uncertain. Therefore, the outdoor gamma radiation dose rate in both seasons is included in this study. Table 2 displays the average, minimum, maximum, standard deviation, and median values of outdoor gamma radiation dose rate. Outdoor gamma radiation dose rate in Anand, Bharuch, Vadodara, and Narmada districts in summer ranged between 74 and 278 nSv/h, 46 and 245 nSv/h, 48 and 287 nSv/h, and 66 and 210 nSv/h, respectively. During the winter season, the gamma radiation dose rate values in Anand, Bharuch, Vadodara, and Narmada districts ranged between 74 and 287 nSv/h, 40 and 278 nSv/h, 19 and 287 nSv/h, and 40 and 210 nSv/h, respectively. The mean value of the outdoor gamma radiation dose rate was somewhat lower in the summer season compared to the winter season; Anand (summer = 149 nSv/h, winter = 150 nSv/h), Bharuch (summer = 125 nSv/h, winter = 131 nSv/h), Vadodara (summer = 147 nSv/h, winter = 158 nSv/h), and Narmada (summer = 128, winter = 128 nSv/h); which is similar as reported in Balod, Chhattisgarh; At-Taif City; Al-Hada Village; and Ash-Shafa Village from the region of Kingdom of Saudi Arabia and three locations from Norway (Al Ghorabie 2005; Mrdakovic et al. 2012; Jindal et al. 2021).

Table 2 Statistical overview of gamma radiation dose rate data from Anand, Bharuch, Vadodara, and Narmada districts of Gujarat State, India

Seasons	Statistical parameters	Gamma radiation dose (nSv/h)			
		Anand	Bharuch	Vadodara	Narmada
	Number of samples	82	144	125	88
Summer	Average	149	125	147	128
	Min	74	46	48	66
	Max	278	245	287	210
	Std. deviation	43	37	42	32
	Median	143	118	143	126
Winter	Average	150	131	158	128
	Min	74	40	19	40
	Max	287	278	287	210
	Std. deviation	43	39	50	37
	Median	139	126	160	126

The exact permissible or threshold value of outdoor gamma radiation dose rate is not available, only prediction of possibility is reported based on epidemic data which is highly uncertain. UNSCEAR (2000) reported the world populated weight average value of radiation dose is 84 nGy h^{-1} and national averages to be in the range 20 to 200 nSv/h. In the present study, out of 439 locations under study, gamma radiation dose rate values from 34 locations in summer and 47 locations in winter exceeded the dose rate of 200 nSv/h. The control charts of gamma radiation dose rate for summer and winter seasons are shown in Fig. 3 which shows the data between range 20 to 200 nSv/h and deviation of data from this range. High radiation dose rate data was obtained in winter season in all districts except Bharuch district. The number of sample locations along with their percentage

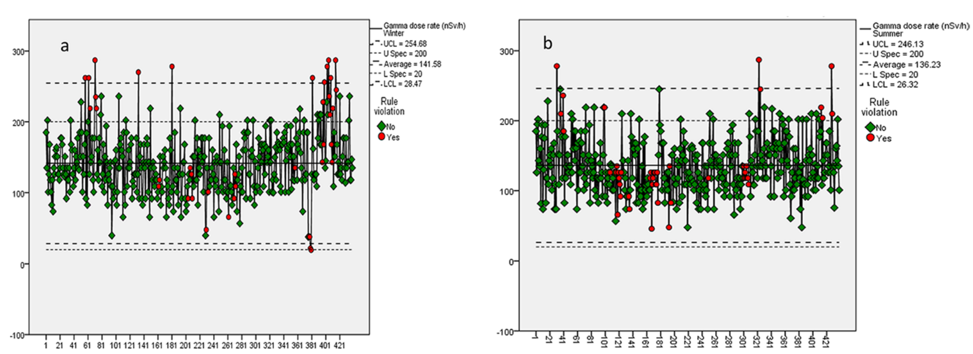

Fig. 3 Control charts for gamma radiation dose rate (nSv/h). **a** Summer. **b** Winter

where gamma radiation dose rate was higher than the 200 nSv/h is shown in Table 3.

AED

Annual effective dose equivalent values for gamma radiation dose rate during summer and winter seasons are given in Table 4. In summer season, the values of AED for Anand, Vadodara, Bharuch, and Narmada districts were found to be 0.09–0.35 mSv/year, 0.06–0.30 mSv/year, 0.08–0.26 mSv/year, and 0.06–0.35 mSv/year, respectively, while in winter, the values were in the range of 0.09–0.35 mSv/year, 0.05–0.34 mSv/year, 0.05–0.26 mSv/year, and 0.02–0.35 mSv/year, respectively. The average values in Anand, Vadodara, Bharuch, and Narmada districts in summer were 0.18 mSv/year, 0.15 mSv/year, 0.16 mSv/year, and 0.18 mSv/year, respectively, and in winter 0.18 mSv/year, 0.16 mSv/year, 0.16 mSv/year, and 0.19 mSv/year, respectively. However, UNSCEAR has reported the worldwide annual average cosmic radiation dose at sea level to be 0.078 mSv/year (with 0.2 occupancy factor of 0.39 mSv/year) and the world populated weighted annual average value of outdoor terrestrial radiation dose was 0.07 mSv/year (UNSCEAR 2000). According to this analysis, all districts' AED values were slightly higher than the aforementioned global average (0.148 mSv/year). The present study being the first of its kind in these regions, the results will provide as essential background information for the area.

Table 3 Samples exceeding gamma radiation dose rate 200 nSv/h in each district

Name of districts (locations)	Gamma radiation dose rate (nSv/h)			
	Number of samples exceeding 200 nSv/h		% of samples exceeding 200 nSv/h	
	Summer	Winter	Summer	Winter
Anand	9	12	11	14
Bharuch	8	7	6	5
Vadodara	14	25	11	20
Narmada	3	3	3	3

Table 4 Annual effective gamma radiation dose values for Anand, Vadodara, Bharuch, and Narmada districts in summer and winter seasons

Season	Statistical parameters	Annual effective radiation dose (mSv/year)			
		Anand	Bharuch	Vadodara	Narmada
Summer	Average	0.18	0.15	0.16	0.18
	Min	0.09	0.06	0.08	0.06
	Max	0.34	0.30	0.26	0.35
	Std. deviation	0.05	0.05	0.04	0.05
	Median	0.18	0.14	0.15	0.18
Winter	Average	0.18	0.16	0.16	0.19
	Min	0.09	0.05	0.05	0.02
	Max	0.35	0.34	0.26	0.35
	Std. deviation	0.05	0.05	0.05	0.06
	Median	0.17	0.15	0.15	0.20

Spatial distribution of gamma radiation

GIS-based spatial analysis is proving to be a potent technique and an excellent instrument for generating the desired results for the spatial distribution of different environmental components (Burrough and McDonnell 1998; Jasrotia and Kumar 2014). It also aids in the analysis of air quality trends and other types of natural radiation. Numerous research were undertaken utilising remote sensing and GIS techniques to map the spatial distribution of the gamma radiation dose rate in districts level to understand the distribution pattern study within various types of geographical setup (Gnanachandrasamy et al. 2018). Using Arc GIS 10.8 software, geographic analysis was carried out for the current study. These samples were plotted according to their GPS-based coordinates, and GIS interpolation techniques were used to create the contours. The representation of the summer and winter gamma radiation dose rate spatial distribution maps for all four districts Anand, Vadodara, Bharuch, and Narmada are given in Figs. 4, 5, 6, and 7, respectively. No definite trend was observed in the districts under study.

Statistical analysis of data

The mean value of gamma radiation dose rate from 439 spots in the summer season was 136.23 nSv/h with a standard deviation of 39.86; however, the gamma dose rate in the winter season was a little higher, at 141.58 nSv/h with a standard deviation of 44.57 (Table 5).

The correlation and paired study were carried out by using the hypotheses.

> Correlation: $H_{o(r1)}$ and $H_{a(r1)}$. $H_{o(r1)}$: there is no relationship between the gamma radiation dose rate in the summer and winter seasons; $H_{a(r1)}$: there is a relationship between the gamma radiation dose rate in the summer and winter seasons. Paired test: $H_{o(d1)}$ = the season has no considerable influence on the gamma radiation dose rate; $H_{a(d1)}$ = the season has a considerable influence on the gamma radiation dose rate.

Based on the statistical analysis of gamma radiation dose rate data from the summer and winter seasons (Table 6), the significance value for paired sample

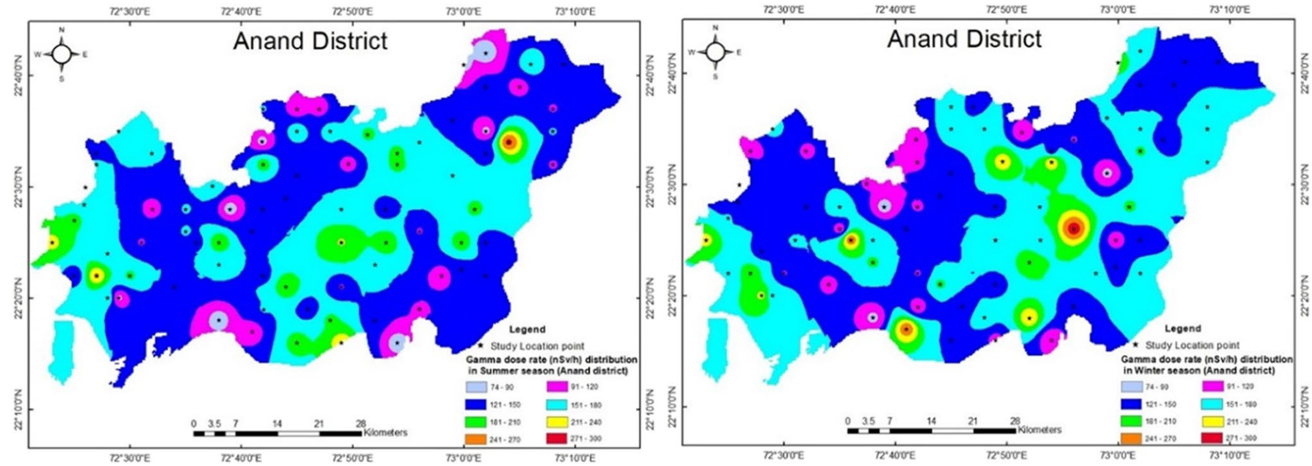

Fig. 4 Gamma radiation dose rate distribution during summer and winter across Anand district

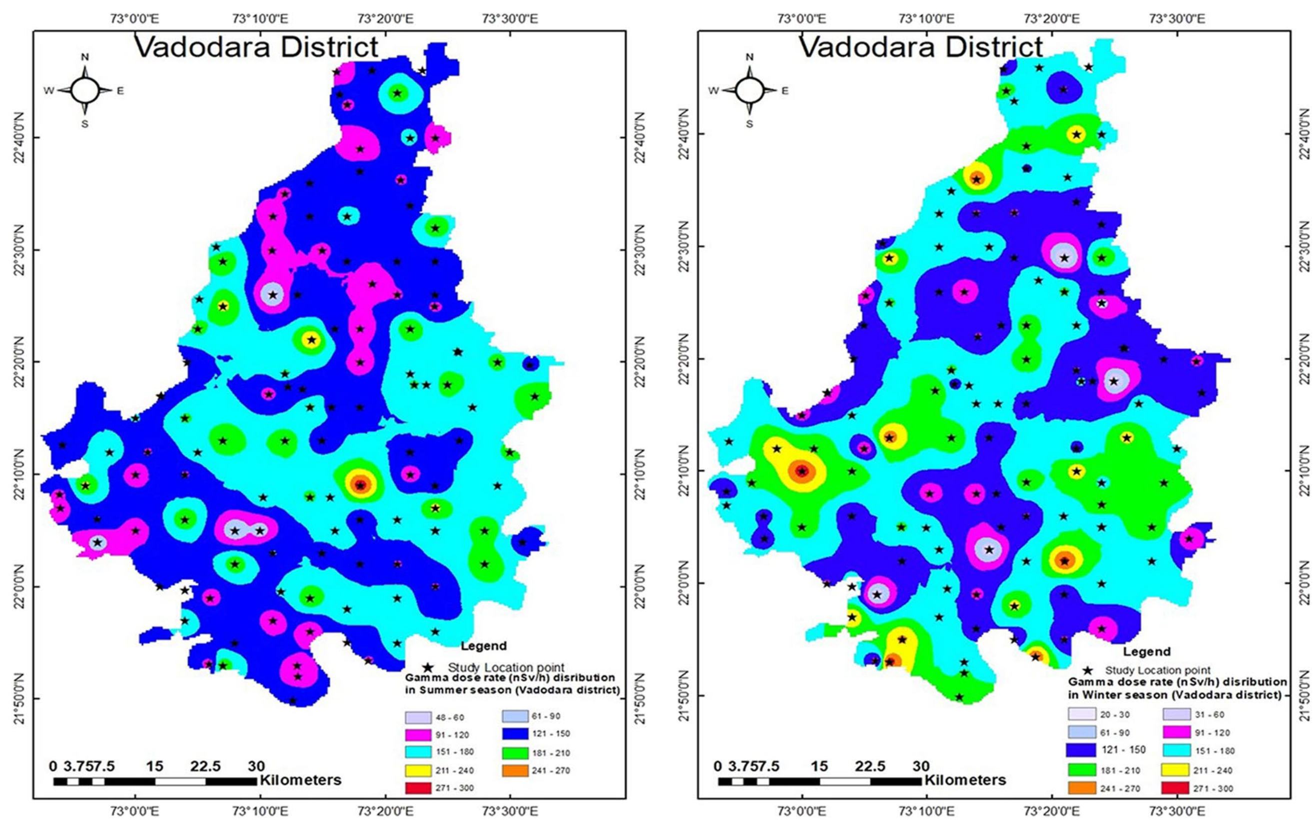

Fig. 5 Gamma radiation dose rate distribution during summer and winter across Vadodara district

correlation between gamma radiation dose rate in the summer and winter seasons was 0.06, which was greater than the 0.05, indicating that the null hypothesis for the study is accepted, revealing that the relationship between gamma radiation dose rate in the summer and winter seasons is not significant. This is also reflected in the correlation value, which is only 0.09; so, monitoring of gamma radiation dose rate is required in both summer and winter.

The significance value of the paired sample *t*-test between outdoor gamma radiation dose rate in summer and winter seasons was 0.05 (Table 7), implying that the null hypothesis for the study is rejected, indicating that seasons have a substantial influence on gamma radiation dose rate. Similar studies

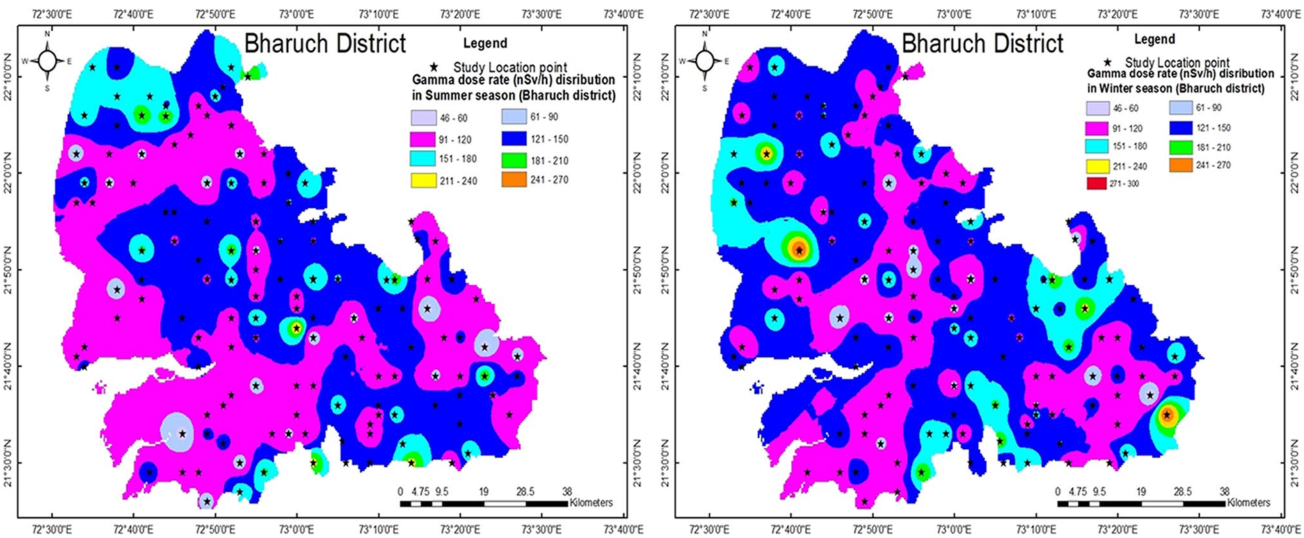

Fig. 6 Gamma radiation dose rate distribution during summer and winter across Bharuch district

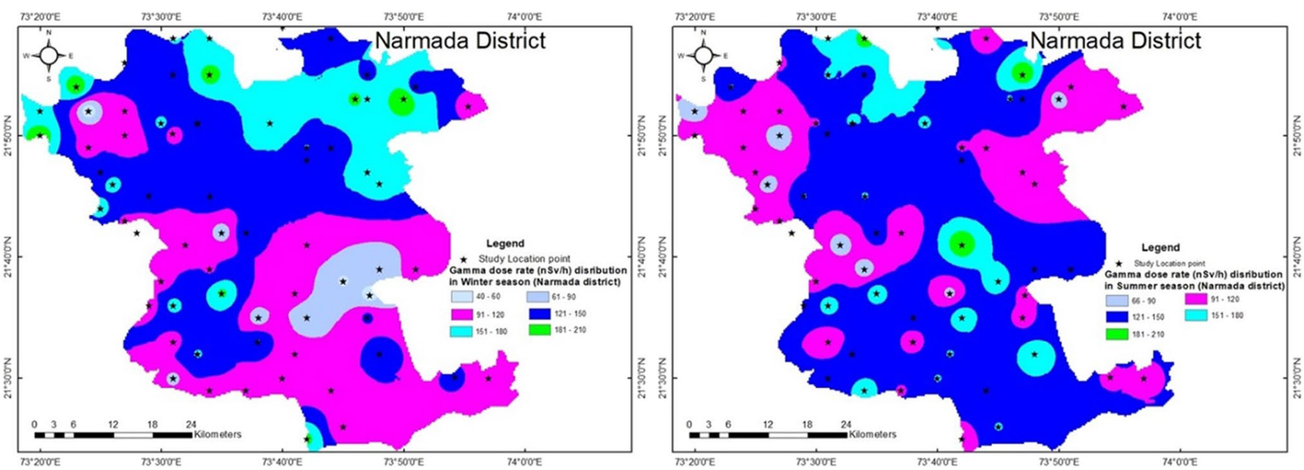

Fig. 7 Gamma radiation dose rate distribution during summer and winter across Narmada district

were reported by various researchers (Jindal et al. 2021). This test also demonstrated the importance of seasonal monitoring. One of the main elements for natural background gamma radiation dose rate is the lithology of the research areas. Ten types of lithology are available in all studied 439 locations with percentage coverage being Alluvium, blown sand, miliolite sand (54.4%); Alluvium, blown sand, miliolite sand, shale, marls and sandstone, limestone, gypsiferous pyritous and carbonaceous shale, Basalt andesite and trachytic flows (6.2%); Alluvium, blown sand, miliolite sand, basalts (Deccan traps) (1.8%); Alluvium, blown sand, miliolite sand, shale, marls and sandstone, limestone, gypsiferous pyritous and carbonaceous shale (2.7%); Alluvium, blown sand, miliolitic sand, Basalt andesite and trachytic flows (6.4%); Alluvium, blown sand, miliolitic sand, Basalt andesite and trachytic flows, Phyllites with mangeniferous horizon, mica-schist and quartzite,

Table 5 Statistics of gamma radiation dose rate in summer and winter seasons

	Mean	*N*	Std. deviation	Std. error mean
Gamma radiation dose rate (nSv/h) summer	136.23	439	39.86	1.90
Gamma radiation dose rate (nSv/h) winter	141.58	439	44.57	2.13

Table 6 Paired samples correlations between gamma radiation dose rate in summer and winter seasons

		N	Correlation	Sig
Pair 1	Gamma radiation dose rate (nSv/h) summer and winter	439	0.09	0.06

Table 7 Paired samples test of gamma radiation dose rate between summer and winter seasons

		Paired differences					*t*	df	Sig. (2-tailed)
		Mean	Std. deviation	Std. error mean	95% confidence interval of the difference				
					Lower	Upper			
Pair 1	Gamma radiation dose rate (nSv/h) summer–winter	− 5.35	57.07	2.72	− 10.71	0.00	− 1.97	438	0.05

limestone, nodular marls and sandstone, quartzite with intercalated phyllites and basal conglomerates, granitoids and pegmatites (4.6%); Basalts (Deccan traps) (9.8%); Limestones and Sandstones (Bagh group) and Basalt (Deccan traps) (7.7%); Limestones and Sandstones (Bagh group) and Quaternary alluvium (2.5%) and; shale, marls and sandstone, limestone, gypsiferous pyritous and carbonaceous shale, Basalt andesite and trachytic flows (3.9%).

Hypotheses study was performed to find the relationship and difference with lithology and gamma radiation dose rate in summer and winter seasons which are as:

Correlation: paired 2: $H_{o(r2)}$: there is no relationship between the gamma radiation dose rates in the summer with lithology; $H_{a(r2)}$: there is a relationship between the gamma radiation dose rates in the summer with lithology. Paired 3: $H_{o(r3)}$: there is no relationship between the gamma radiation dose rates in the winter with lithology; $H_{a(r3)}$: there is a relationship between the gamma radiation dose rates in the winter with lithology. Differences: paired 2: $H_{o(d2)}$ = the lithology had no considerable influence on the gamma radiation dose rate in summer season; $H_{a(d2)}$ = the lithology had a considerable influence on the gamma radiation dose rate in summer season. Paired 3: $H_{o(d3)}$ = the lithology had no considerable influence on the gamma radiation dose rate in winter season; $H_{a(d3)}$ = the lithology had a considerable influence on the gamma radiation dose rate in winter season.

SPSS software was used for statistical analysis by converting the lithology string data to numeric data. The correlation analysis (Table 8) indicated that the pair 2 gamma radiation dose rate in summer with lithology followed the null hypothesis, while pair 3 indicated that the analysis

Table 8 Paired samples correlation for gamma radiation dose rate in summer and winter with lithology of the study locations

		N	Correlation	Sig
Pair 2	Gamma radiation dose rate (nSv/h) summer and lithology	439	− 0.08	0.08
Pair 3	Gamma radiation dose rate (nSv/h) winter and lithology	439	− 0.13	0.00

Table 9 Paired samples test for gamma radiation dose rate with lithology of the areas in summer and winter seasons

		Paired differences					*t*	df	Sig. (2-tailed)
		Mean	Std. deviation	Std. error mean	95% confidence interval of the difference				
					Lower	Upper			
Pair 2	Gamma radiation dose rate (nSv/h) summer–lithology	132.88	40.23	1.92	129.11	136.66	69.21	438	0.00
Pair 3	Gamma radiation dose rate (nSv/h) winter–lithology	138.24	45.08	2.15	134.01	142.46	64.25	438	0.00

Table 10 Statistical analysis of gamma radiation dose rate with lithology of the areas

		Alluvium, blown sand, miliolite sand	Alluvium, blown sand, miliolite sand, shale, marls and sandstone, limestone, gypsiferous pyritous	Alluvium, blown sand, miliolite sand, basalts (Deccan traps)	Alluvium, blown sand, miliolite sand, shale, marls and sandstone, limestone, gypsiferous pyritous and carbonaceous shale	Alluvium, blown sand, miliolitic sand, basalt andesite and trachytic flows	Alluvium, blown sand, miliolitic sand, basalt andesite and trachytic flows, phyllites with mangeniferous horizon, mica-shale	Basalts (Deccan traps)	Limestones and sandstones (Bagh group) and basalt (Deccan traps)	Limestones and sandstones (Bagh group) and quaternary alluvium	Shale, marls and sandstone, limestone, gypsiferous pyritous and carbonaceous shale, basalt andesite and trachytic flows
Gamma radiation dose rate (nSV/h) summer	Min	48	46	74	83	92	48	74	66	101	92
	Max	287	202	210	219	210	202	202	210	194	219
	Mean	141.05	115.41	128.13	125.25	147.96	135.5	128.95	122.88	143.55	134.88
	Median	135	109	119.5	113.5	147	135	126	118	135	126
	Std. deviation	41.92	36.05	45.75	42.73	38.63	42.14	29.32	34.63	30	33.73
	Skewness	0.7	0.56	0.78	1.27	0.04	−0.13	0.14	0.82	0.22	0.8
	Kurtosis	0.71	1.37	0.01	0.75	−1.35	−0.12	−0.32	0.85	−1.17	0.91
	Range	239	156	136	136	118	154	128	144	93	127
Gamma radiation dose rate (nSV/h) winter	Min	66	66	126	83	101	19	48	40	101	40
	Max	287	219	210	202	210	262	185	210	177	270
	Mean	147.5	133.26	146	138.75	156.11	122.97	112.49	143.47	144.55	137.29
	Median	143	135	130.5	136	160.5	126	109	139	151	126
	Std. deviation	44.78	38.5	30.06	40.88	33.78	69.99	32.77	36.79	28.07	54.71
	Skewness	0.91	0.57	1.68	0.07	−0.02	0.21	0.41	−0.27	−0.5	0.59
	Kurtosis	0.87	0.51	2.52	−1.52	−1.17	−0.48	−0.16	0.56	−1.06	0.91
	Range	221	153	84	119	109	243	137	170	76	230

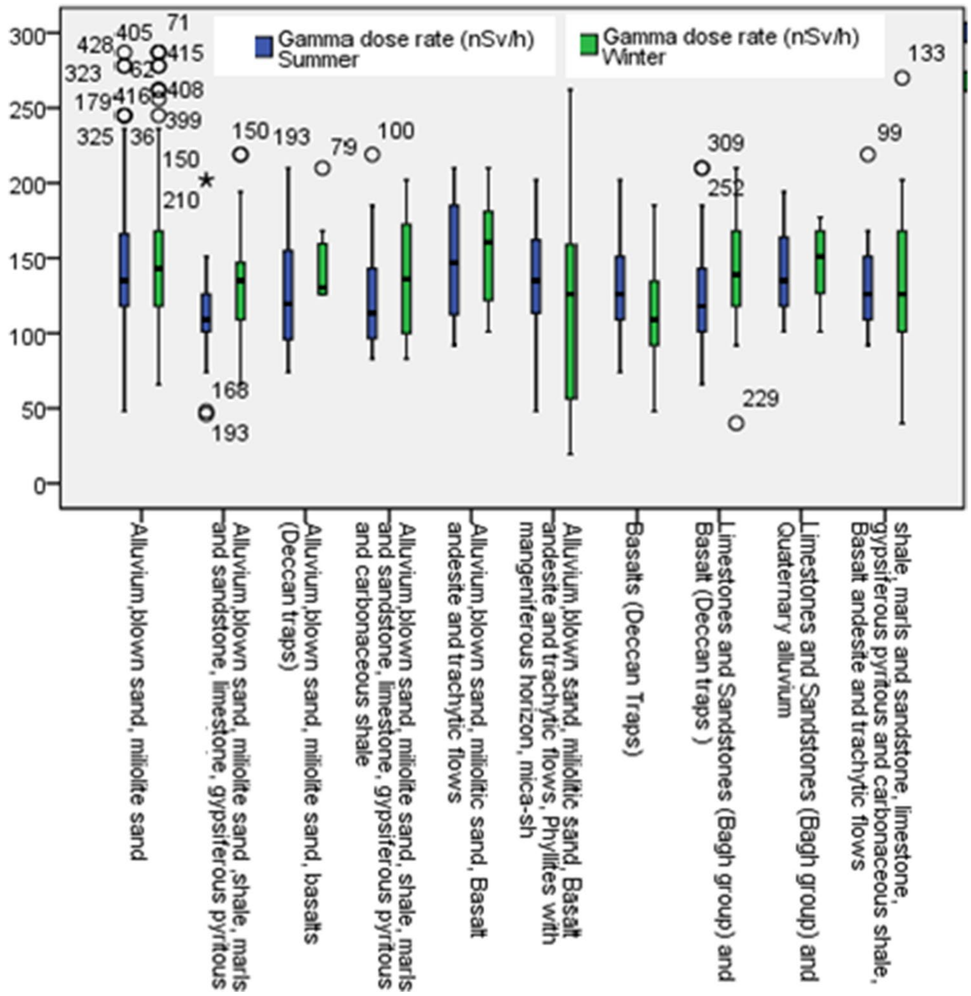

Fig. 8 Box plot of gamma radiation dose rate based on lithology in summer and winter seasons

followed the alternative hypothesis in some way. There was no significant relationship between lithology and gamma radiation dose rate in the summer season, however, statistical study indicates that there was a significant relationship between lithology and gamma radiation dose rate in the winter season.

The paired difference test was used to determine the statistical difference in gamma radiation dose rate in the summer and winter seasons along with the lithology of the studied areas. The paired sample *t*-test significance values for gamma radiation dose rate in summer and winter seasons with lithology were zero (Table 9), implying that the null hypothesis for the study is accepted, demonstrating that lithology has no significant impact on gamma radiation dose rate.

Table 10 shows the statistical results of gamma radiation dose rate for summer and winter, as well as the box plot in Fig. 8 for summer and winter based on lithology of study area. It was observed that the measured gamma radiation dose rates from summer and winter are found in a very wide range. The variation observed in all districts may be due to several types of geological and lithological variations.

From this study, it was observed that area comprising (Alluvium, blown sand, miliolite sand) of lithology are showing high frequency of gamma radiation dose rate in the study area. Figure 9 represents frequency distribution of gamma radiation dose rate in both seasons on the basis of lithology. From the figure, it is also observed that basaltic rocks are also responsible for high gamma radiation dose rate. Some researchers also have studied gamma radiation dose rate on the basis of lithological formation (Adabanija et al. 2020).

Conclusion

Gamma radiation dose levels were monitored in four districts of Gujarat, India: Anand, Bharuch, Vadodara, and Narmada. Many radionuclides emit gamma radiation; some have short half-lives, while others have very long

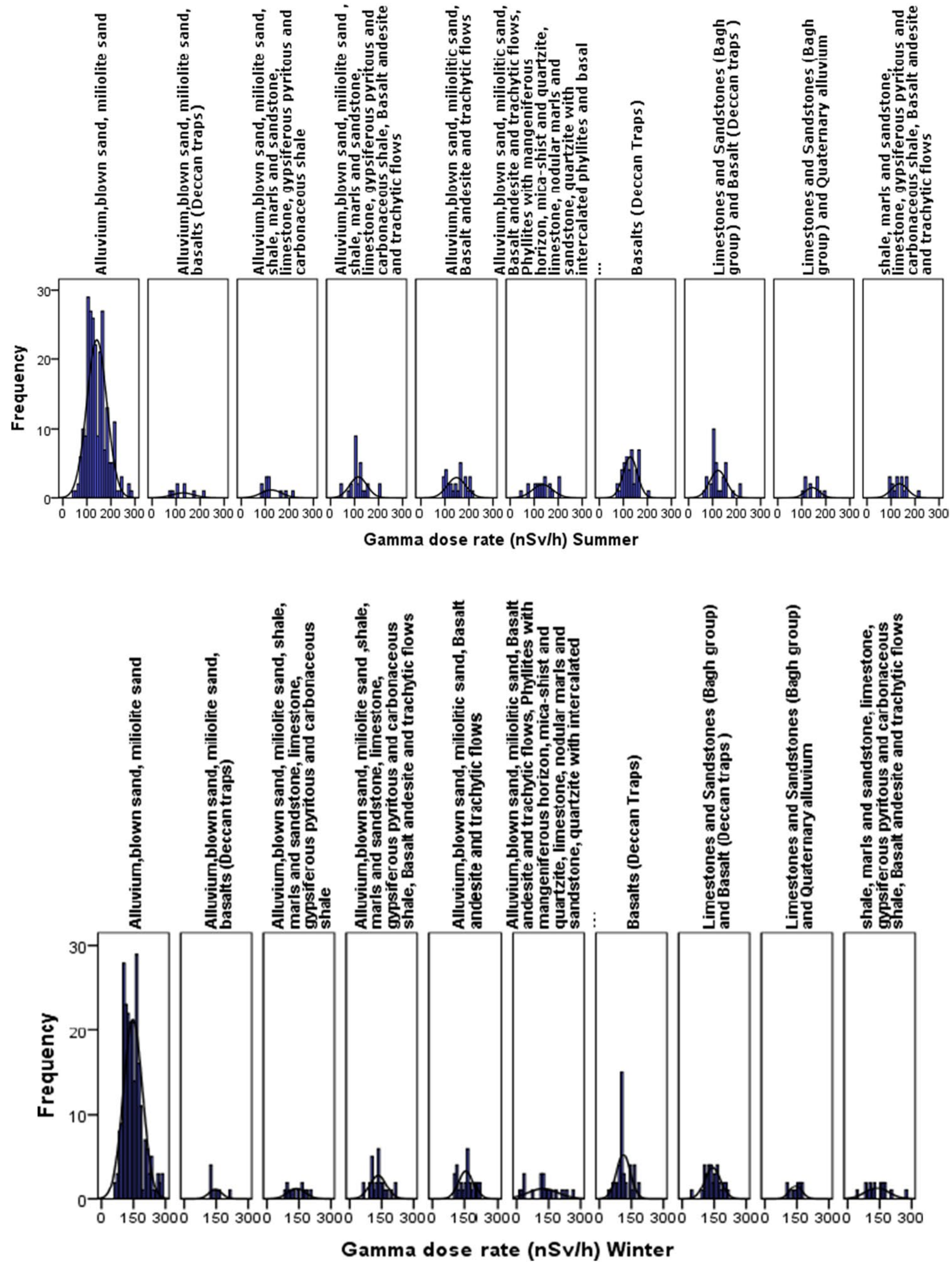

Fig. 9 Frequency of gamma radiation dose rate (nSv/h) based on lithology in summer and winter seasons

half-lives. It is constantly decaying and emitting gamma radiation into the environment. The findings from this investigation showed that the mean value of the outdoor gamma radiation dose rate was slightly lower in the summer than in the winter. The mean values of gamma radiation dose rate in Anand, Bharuch, Vadodara, and Narmada districts in the summer season were 149, 125, 147, and 128 nSv/h, respectively, while in winter, the values were 150, 131, 158, and 128 nSv/h, respectively. The results demonstrated that the gamma radiation dose rate exceeded the value of 200 nSv/h by 8 and 11% in the summer and winter seasons, respectively. The geographical spatial distribution of gamma radiation dose rate for all four districts can be useful for other radionuclides studies. Annual effective dose values were found to be greater than the world average value reported by UNSCEAR. There was no significant relationship between lithology and gamma radiation dose rate in the summer season, while a significant relationship between lithology and gamma radiation dose rate was observed in the winter season. The significant relationship between lithology and gamma radiation dose rate may be attributed to the exposure of lithology of the area and leaching of the radioactive materials during the rains occurring just before winter season than in summer. According to statistical analysis, the variations in gamma radiation dose rate with lithology in the summer and winter seasons also support the notion that the radiation dose is higher in the winter season. The study will be useful in comprehending and averting risk that arises in future from radiation or radionuclides in these areas.

Acknowledgements PPS, DC, and DP acknowledge the Board of Research in Nuclear Sciences for funding this project.

Author contribution Project inception and management was done by PPS and DC. DC, PPS, and DP contributed to the experimental design and collection of samples. Data analysis was done by DC, PPS, DP, and MKJ. The first draft of the manuscript was written by DP and MKJ, and all authors commented on previous versions of the manuscript and modified the manuscript. All authors read and approved the final manuscript.

Funding This study was funded by the Board of Research in Nuclear Sciences (BRNS), DAE sanction number 36(4)/14–77-2014/BRNS/10084 under NUP.

Data availability The datasets generated during and/or analysed during the current study are available from the corresponding author on reasonable request.

Declarations

Ethics approval and consent to participate Not applicable.

Consent for publication Not applicable.

Conflict of interest The authors declare no competing interests.

References

Adabanija M, Anie O, Oladunjoye M (2020) Radioactivity and gamma ray spectrometry of basement rocks in Okene area, southwestern Nigeria. NRIAG J Astron Geophys 9:71–84

Al-Ghorabie FHH (2005) Measurements of environmental terrestrial gamma radiation dose rate in three mountainous locations in the western region of Saudi Arabia. Environ Res 98:160–166

Almayahi BA, Tajuddin AA, Jaafar MS (2012) Radiation hazard indices of soil and water samples in northern Malaysian Peninsula. Appl Radiat Isot 70:2652–2660

Anand District Administration (2022), Government of Gujarat. https://anand.nic.in Accessed 15th May 2022

Bharuch District Administration (2022), Government of Gujarat. https://bharuch.nic.in Accessed 5th April 2022

Burrough PA, McDonnell RA (1998) Principles of Geographical Information Systems. Oxford University Press, Oxford

CGWB (2014) Groundwater brochure Narmada District. Government of India Ministry of Water Resources

Cooper MB (2005) Naturally occurring radioactive materials (NORM) in Australian industries-review of current inventories and future generation. Report ERS-006 (EnviroRad Services Pty. Ltd.) to the Radiation health and Safety Advisory Council

Dhawal SJ, Phadatare MR, Thorat ND, Kulkarni GS, Pawar SH (2013) Natural radioactivity study in soil samples of south Konkan, Maharashtra, India. Radiat Prot Dosimetry 157:225–233

GCWB (2014) Groundwater brochure, Bharuch District. Technical Report Series. Government of India, Ministry of Water Resources, Central Ground Water Board West Central Region, Ahmedabad

Gnanachandrasamy G, Zhou Y, Bagyaraj M, Venkatramanan S, Ramkumar T, Wang S (2018) Remote sensing and GIS based groundwater potential zone mapping in Ariyalur District, Tamil Nadu. J Geol Soc India 92:484–490

Guarino A, Cicchella D, Lima A, Albanese S (2022) Radon flux estimates, from both gamma radiation and geochemical data, to determine sources, migration pathways, and related health risk: the Campania region (Italy) case study. Chemosphere 287:132233

Gupte PR (2012) Review of aquifer system of Deccan trap area, Gujarat state. In Fifth IGWC-2012-TS-1-93, Conference: International Ground Water Congress

Gusain GS, Rautela BS, Sahoo SK, Ishikawa T, Prasad G, Omori Y, Sorimachi A, Tokonami S, Ramola RC (2012) Distribution of terrestrial gamma radiation dose rate in the eastern coastal area of Odisha, India. Radiat Prot Dosimetry 152:42–45

Harikrishnan N, Ravisankar R, Chandrasekaran A, Gandhi MS, Vijayagopal P, Mehra R (2018) Assessment of gamma radiation and associated radiation hazards in coastal sediments of south east coast of Tamilnadu, India with statistical approach. Ecotoxicol Environ Saf 162:521–528

Imani M, Adelikhah M, Shahrokhi A, Azimpour G, Yadollahi A, Kocsis E, Toth BE, Kovács T (2021) Natural radioactivity and radiological risks of common building materials used in Semnan Province dwellings, Iran. Environ Sci Pollut Res 28:41492–41503

Jasrotia AS, Kumar A (2014) Groundwater quality mapping based on the Geographical Information System (GIS) of Jammu District, Jammu and Kashmir India. J Spat Hydrol 12(1)

Jindal MK, Sar SK (2020a) Statistical comparative study of the gamma dose rate and associated risk assessment in rural and urban areas of Durg District, Chhattisgarh, India. Radiochemistry 62:275–287

Jindal MK, Sar SK (2020b) Blueprint of indoor gamma dose rate through statistical modelling for Kabirdham District. J Radioanal Nucl Chem 325:121–131

Jindal MK, Sar S, Arora A, Singh S, Sahu M, Diwan V (2018a) Annual effective dose equivalent of population staying in industrial area Bhilai, Chhattisgarh India estimated using gamma dose rate measurements. Res J Chem Environ 22:22–27

Jindal MK, Sar SK, Singh S, Arora A (2018b) Risk assessment from gamma dose rate in Balod District of Chhattisgarh, India. J Radioanal Nucl Chem 317:387–395

Jindal MK, Sar SK, Baghel T, Wadhwa DS (2021) Statistical study of the factors affecting outdoor gamma dose rate and impact of season. J Geol Soc India 97:85–93

Karunakara N, Yashodhara I, Kumara KS, Tripathi RM, Menon SN, Kadam S, Chougaonkar MP (2014) Assessment of ambient gamma dose rate around a prospective uranium mining area of south India-a comparative study of dose by direct methods and soil radioactivity measurements. Results Physics 4:20–27

Mrdakovic PJ, Bhatt CR, Salbu B, Skipperud L (2012) Outdoor ^{220}Rn, ^{222}Rn and terrestrial gamma radiation levels: investigation study in the thorium rich fen complex, Norway. J Environ Monit 14:193–201

Nandkeolyar N, Sandhya Kiran G (2019) A climatological study of the spatio-temporal variability of land surface temperature and vegetation cover of Vadodara district of Gujarat using satellite data. Int J Remote Sens 40(1):218–236

Narmada District Administration (2022) Government of Gujarat. https://narmada.nic.in Accessed 15th April 2022

Negi MS, Prasad Y, Prasad G, Gusain GS, Badoni M, Ramola RC (2009) Gamma radiation dose rate in indoor, outdoor and underground atmosphere around Tehri Dam Project, Uttarakhand, India. Indian J Phys 83:1209–1214

NRC (2006) Health risks from exposure to low levels of ionizing radiation: BEIR VII phase 2. The National Academies Press, Washington, DC

Omori Y, Sorimachi A, Gun AM, Enkhgerel N, Munkherdene G, Oyunbolor G, Shajbalidir A, Palam E, Yamada C (2019) Gamma dose rate distribution in the Unegt subbasin, a uranium deposit area in Dornogobi Province, southeastern Mongolia. Environ Sci Pollut Res 26:33494–33506

Patel D, Padmaja SP, Chakraborty D, Akhilesh Y (2022) Bharuch District, Gujarat, India: factor analysis and geographical distribution of water quality characteristics. Environ Nanotechnol Monit Manag 18:100732

UNSCEAR (United Nations Scientific Committee on the Effects of Atomic Radiation) (2000) Effects of ionizing radiation. United Nations, New York, pp 453–487

Yadav SS (2013) Technical Report Series, District groundwater brochure-Anand District Gujarat. Central Groundwater Board, Ahmedabad

Yu KN, Guan ZJ, Stokes MJ, Young ECM (1992) The assessment of the natural radiation dose committed to the Hong Kong people. J Environ Radioact 17:31–48

Publisher's note Springer Nature remains neutral with regard to jurisdictional claims in published maps and institutional affiliations.

Groundwater for Sustainable Development 24 (2024) 101050

Contents lists available at ScienceDirect

Groundwater for Sustainable Development

journal homepage: www.elsevier.com/locate/gsd

Research paper

Groundwater quality evaluation of Narmada district, Gujarat using principal component analysis

Divya Patel [a], Padmaja Pamidimukkala [a,b,*], Debjani Chakraborty [b]

[a] Department of Environmental Studies, The Maharaja Sayajirao University of Baroda, Vadodara, Gujarat, India
[b] Department of Chemistry, The Maharaja Sayajirao University of Baroda, Vadodara, Gujarat, India

HIGHLIGHTS

- Physicochemical characteristics of Narmada district ground water was monitored.
- Water Quality Index was used to evaluate the quality of ground water.
- The quality was associated with geogenic processes and mineral deposits.
- Principal Component Analysis and Correlation analysis were applied to the data.
- Tilakwada ground water was found to be unsuitable for drinking purposes.

GRAPHICAL ABSTRACT

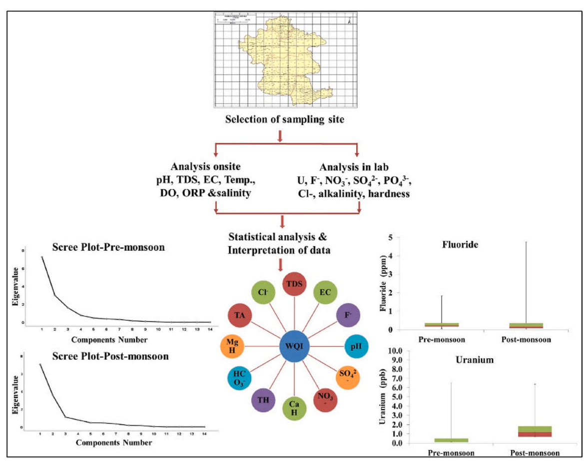

ARTICLE INFO

Keywords:
Fluoride
Uranium
Groundwater quality index
Principal component analysis

ABSTRACT

In the present study, the ground water quality parameters were monitored during pre- and post-monsoon seasons across Narmada district, Gujarat, India. Monitoring was done in 89 drinking water samples collected by grid sampling method from the study area. Uranium and fluoride were analyzed along with associated parameters such as pH, dissolved oxygen, Cl^-, NO_3^-, F^-, SO_4^{2-}, total alkalinity, total dissolved solids and hardness. In 4% samples the fluoride content was found to be above WHO permissible limits of 1.5 mg/L (2.36 mg/L in Undaimandava, 1.55 mg/L in Shira, 3.04 mg/L in Fatehpur and 1.83 mg/L in Dholivav) during pre-monsoon season (PRM) and 4.74 mg/L, 2.41 mg/L, 2.34 mg/L and 3.99 mg/L respectively in Bantawadi, Shira, Undai Mandava and Fatepur villages during post-monsoon (POM). The uranium level was within WHO limits in both POM and PRM seasons. The quality of the water was evaluated by Principal Component and Pearson Correlation statistical analysis techniques. The PRM and POM correlation study indicated a strong correlation of TDS with EC, Chloride, total alkalinity and bicarbonate and U while moderately strong correlation of TDS with fluoride were observed indicating that chloride, total alkalinity, bicarbonate, U and fluoride contributed to TDS and EC. Principal component analysis was applied for 14 variables, from which 3 factors were extracted during PRM and

* Corresponding author: Department of Chemistry, The Maharaja Sayajirao University of Baroda, Vadodara, Gujarat, India.
E-mail address: padmaja.sudhakar-chem@msubaroda.ac.in (P. Pamidimukkala).

https://doi.org/10.1016/j.gsd.2023.101050
Received 12 July 2022; Received in revised form 1 October 2023; Accepted 21 November 2023
Available online 27 November 2023

POM seasons. The extracted components, contributed 84.391% and 83.315%, to variation during PRM and POM seasons respectively. The study indicated that the analyzed water samples in Narmada district were safe for drinking purpose. However, Tilakwada tehsil groundwater was observed to be unsustainable for drinking, without further water treatment, but was appropriate for agricultural purposes. The study will help the residents of the district to understand the present water quality status and will also help in future management to protect the ground water of Narmada district.

1. Introduction

Water is indispensable for sustenance of life(Hossain et al., 2022). Inadequate water supply is still one of the major challenges across the globe. Due to overexploitation of groundwater for irrigation, industrial use, and other factors such as less rainfall, hot temperature, high surface runoff in hilly areas and climate change (leads to low natural recharge of aquifers), groundwater table has been falling all over the region (Hossain et al., 2021). Kafy et al. observed that land cover/land use affected the groundwater chemistry (Kafy et al., 2021). The minerals in the rocks and sediments dissolve in groundwater to varying degrees as the water comes in contact with the rocks and sediments. The extent of dissolution dictates the applicability of water for various purposes (Patil et al., 2010). A worldwide push to monitor groundwater quality and identify safe and sustainable water resources has resulted from the increasing demand on aquifers for water supply and the effects of human activity on aquifers. Physicochemical parameters that affect potability of groundwater include hardness, alkalinity, TDS, salinity and chloride, sulphate, nitrate content etc. Presence of these parameters beyond permissible limits makes the water unfit for potable purposes (WHO, 2011; Arulnangai et al., 2021). Occurrence of fluoride in groundwater is one of the major problems across the world notably in United States of America, Africa and Asia (Battaleb-Looie et al., 2012). In India fluoride contaminated groundwater is mainly prevalent in arid and semi-arid regions viz, Uttar Pradesh, Rajasthan, Haryana, Punjab, Gujarat, Andhra Pradesh, Assam, Bihar, Chhattisgarh, Delhi, Karnataka, Madhya Pradesh, Maharashtra, Odisha, Rajasthan and West-Bengal (Battaleb-Looie et al., 2012; Ali et al., 2019; Keesari et al., 2021). Fluoride is a geogenic pollutant dependent on the types of fluoride mineral bearing rocks, hydro geological strata, presence of other ions particularly bicarbonate and calcium and time of contact between rock and groundwater. Agricultural and industrial activities also contribute to ground water contamination (Ali et al., 2019).

Uranium, a lithophilic naturally occurring radioactive actinide is another geogenic pollutant with wide variation in concentration (Patra et al., 2013; UNSCEAR, 2016). Further, due to weathering and other

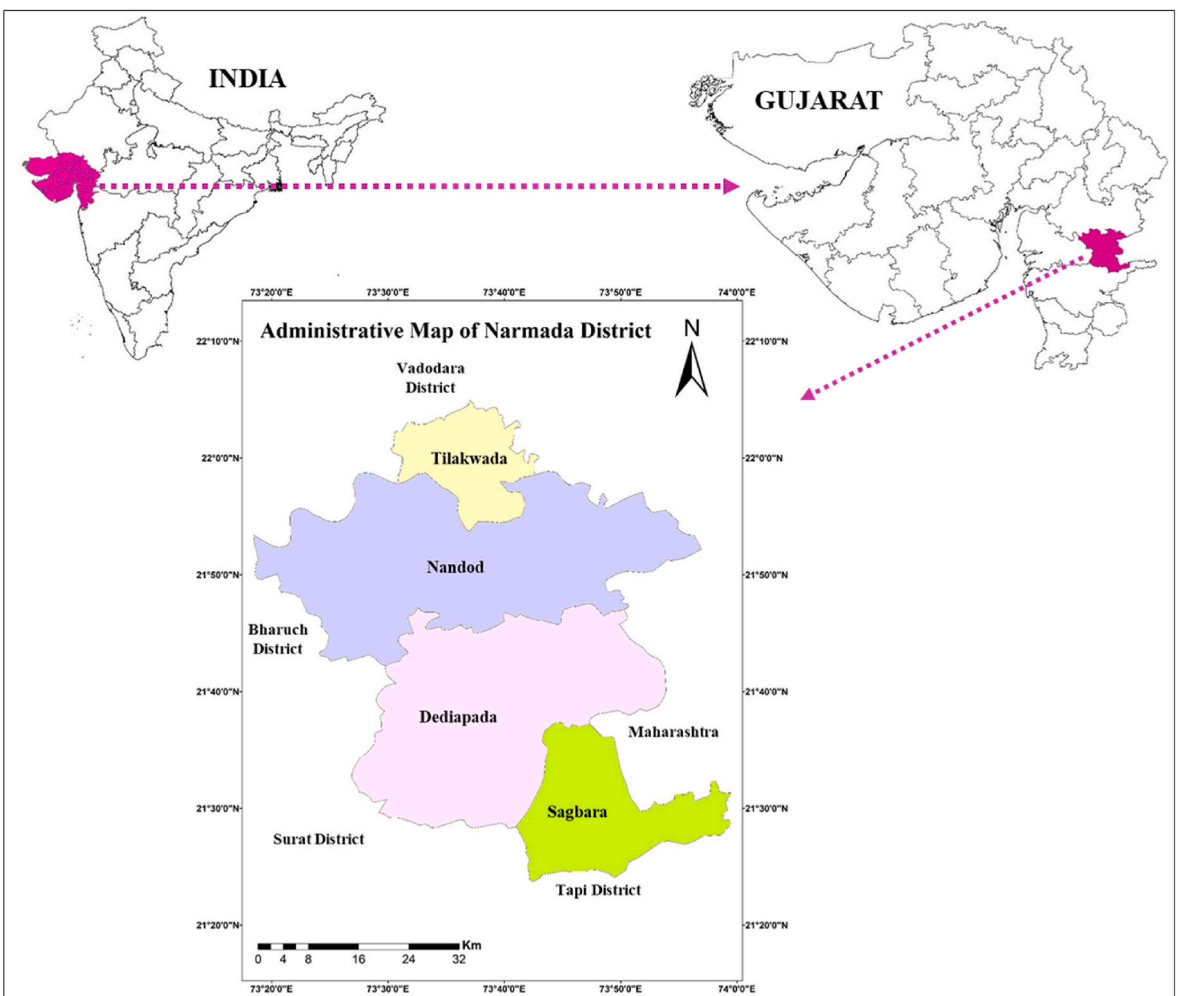

Fig. 1. Map showing study area (Narmada district, Gujarat).

Table 1
Physiography of Narmada district.

Topography	Description
Hilly areas	Rajpipla hills
Piedmont zone	Periphery of hilly area with outward sloping
Alluvial plain	Deposited during the Holocene and Pleistocene period
Drainage	By Narmada, Kim and Tapi rivers

geological processes it leaches to groundwater from host rocks and soils (Pazand, 2016; UNSCEAR, 2016) and depends on physicochemical characteristics of water (Coyte et al., 2018; Sharma et al., 2018). However, modern agriculture practices, mining, ore processing and over exploitation of groundwater, and other anthropogenic activities may further contribute to U contamination in groundwater (Bhalara et al., 2014; Bigalke et al., 2018). Systematic monitoring of uranium contamination in groundwater was done by few researchers (Srivastava et al., 2021; Balaram et al., 2022). Studies in Narmada district, Gujarat is very scarce. A flow model developed by Jain et al. for Narmada River basin aquifers in Gujarat, indicated the water levels to be stable (Jain et al., 2021). The Central Ground Water Board studies were specifically focused on physicochemical groundwater characteristics (CGWB, 2014) rather than uranium and or fluoride evaluation which has been taken up in this study as a part of the National Uranium Project, BARC. In this project, water quality parameters including fluoride and uranium have been systematically monitored throughout India to obtain baseline data \ and understand the spatial distribution of the parameters (Kale et al., 2019; Sharma et al., 2018; Kale et al., 2020; Patni et al., 2020; Sahu et al., 2020; Patel et al., 2022).

In the present study, the objective was to perform pre- and post-monsoon (PRM, POM) physicochemical assay of water including uranium and fluoride content in Narmada district of Gujarat to serve as baseline for future industrialization as well as surrounding industrialized districts. The study also focused on the correlation among the physicochemical parameters through Pearson Correlation Matrix and Principal Component Analysis(PCA).

2. Study area description

Narmada district lies towards south of Gujarat between 21°23′ and 22°05′ north latitudes and 73°17′ and 73°59’ east longitudes, bounded in the north by Vadodara, in the south by Surat, in the west by Bharuch districts and in the east by Maharashtra (Fig. 1). The district comprises of Tilakwada, Nandod, Dediapada and Sagbara tehsils. Among these, Tilakwada tehsil has different geographical and rock properties as compared to other three tehsils under study. Tilakwada tehsil and a small part of Nandod have soft rock aquifers while most part of Nandod, Dediapada and Sagbara have hard rock aquifers (CGWB, 2014).

2.1. Geology and hydrogeology of narmada district

Narmada district has a varied landscape. According to Groundwater brochure Narmada district may be divided into following four topographic units (Table 1).

The study area has no major industries (MSME, 2011), so the main sources of water pollutants are geogenic in origin. Most part of the district has basaltic rocks of the cretaceous age devoid of minerals with deposition of sandstone, limestone, shale and quartzite. The district has soft rock aquifer, hard rock aquifer and hilly area (Fig. 2). Most of the

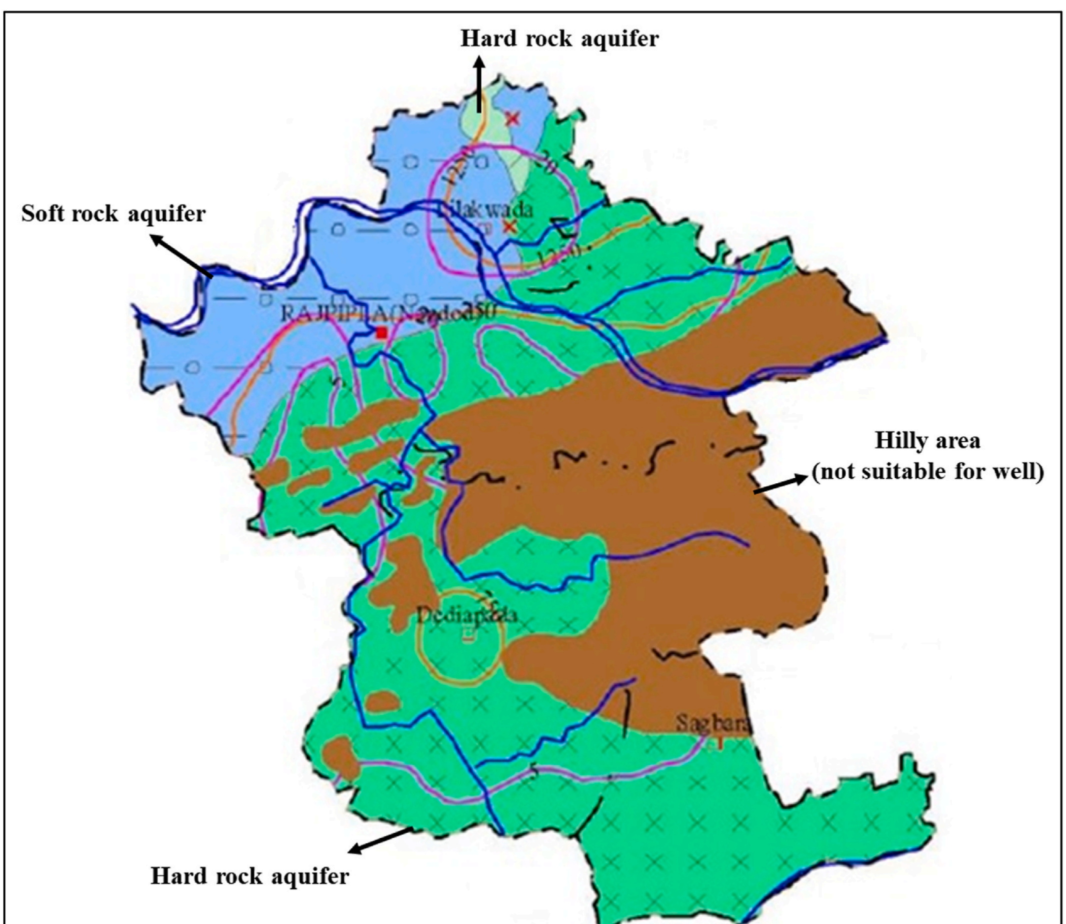

Fig. 2. Hydrogeological conditions of Narmada (CGWB, 2014).

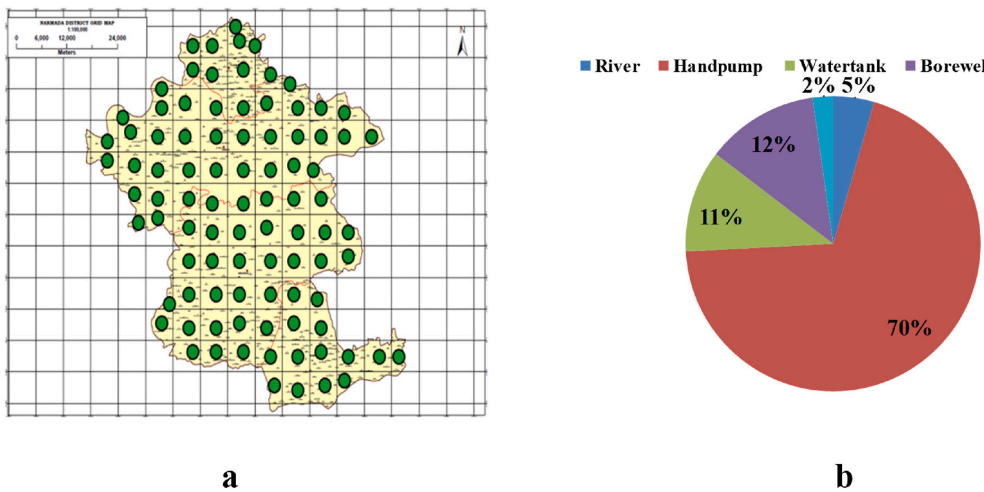

Fig. 3. (a) Sampling points (Green dots) in Narmada District (b) Sources of drinking water across Narmada district (%). (For interpretation of the references to colour in this figure legend, the reader is referred to the Web version of this article.)

district's groundwater occurs underlain in all the rock formations (CGWB, 2014).

The north part of the district through which river Narmada flows is covered by alluvium, gravel and boulders. In the Infratrappean rocks (Bagh beds, sandstone, marls and limestone), groundwater also comprises of water in the pores between sand grains, while the fissures and fractures contribute significantly to the mobility of ground water (CGWB, 2014).

3. Methodology

3.1. Sampling method of groundwater

The groundwater was collected by systematic grid sampling from each of 6 × 6 km square grids (green dots, Fig. 3-a) in Narmada district. A total of eighty-nine samples were collected during both POM and PRM seasons respectively with the help of GPS instrument. The groundwater/drinking water samples collected were from water sources (Fig. 3-b), which were being regularly used by the inhabitants. The water samples was taken from hand pumps and bore wells after letting the water out for about 5 min in pre-cleaned polyethylene bottles rinsed with respective water samples to be collected while in case of open drinking sources such as rivers and wells, the sample was collected directly into the pre-cleaned bottles after rinsing. Water samples were collected in separate bottles for U analysis and were immediately acidified with HNO_3.

All analyses have been performed in triplicate and the standard deviation has been included at appropriate places.

3.2. Estimation of uranium

Uranium was estimated by a calibrated LED-fluorimeter (LF-2) supplied by Quantalase Enterprises Pvt. Ltd, India. To a 10 mL of water sample, 1 mL of 5% $Na_4P_2O_7$ (as a fluorescence enhancer and to maintain a single uranium species) buffered to pH 7 was added. Uranium content in the samples was analyzed using standard addition technique to avoid matrix effect. All samples were analyzed in triplicate and concentration was calculated using the expressions (1) and (2):

$$\textit{Calibration factor} = \frac{\text{Concentration of uranium in standard solution}}{\text{Fluorescence of standard} - \text{Fluorescence of water}} \quad (1)$$

$$\textit{Concentration of uranium} = CF \times (\textit{fluorescence of sample} - \textit{fluorescence of water}) \quad (2)$$

3.3. Assay of ground water F^- content

A fluoride ion selective electrode (A214-model Supplied by Thermo Scientific Orion star) was used to determine F^- concentration in the groundwater samples under study. Calibration standards were prepared from 1000 mgL^{-1} fluoride stock solution. Total ionic strength adjustment buffer (TISAB-III) was used to regulate the ionic concentration as well as pH of samples and standard solutions.

3.4. Associated physicochemical parameter analysis

The quality of groundwater is significantly affected by various water quality parameters. In- situ physicochemical parameters (Total dissolved solid, salinity, electrical conductance, temperature, dissolved oxygen, pH, and redox potential) were analyzed during sampling on site. The groundwater sample analysis of nitrate, phosphate, sulphate was performed in the laboratory using APHA standard methods. Alkalinity was obtained by titration with sulphuric acid and hardness by titration with ethylene diamine tetra acetic acid. The carbonate and bicarbonate hardness as well as Mg hardness were calculated theoretically. Chloride concentration was estimated by Mohr's method (APHA, 2017).

3.5. Correlation matrix studies

The correlation among the parameters under study was investigated using Karl Pearson correlation matrix. The Correlation coefficient (R) among the water quality parameters was calculated using Pearson equation (3):

$$R = \frac{\text{covar}(x, y)}{\sigma x \sigma y} = \frac{\frac{\sum xy}{n} - \left(\frac{\sum x}{n}\right)\left(\frac{\sum y}{n}\right)}{\sigma x \sigma y} \quad (3)$$

where x and y are variables, σx and σy the standard deviations of x and y respectively and covar (x,y) their covariances for n pairs of data sets.

3.6. Water quality index (WQI)

The suitability of groundwater for drinking purposes indicated by WQI, was graded as excellent, good, poor and very poor (Udeshani et al., 2020). Each water quality parameter under study was given a weight (Wi) based on the extent of its contribution to the quality of water. Parameters of major significance were given a maximum weight of '5' while parameters of least significance were given a minimum weight of '2'. Equations (4)–(7) were used in WQI determination.

Table 2
Narmada District groundwater analysis during PRM and POM.

Parameters	PRM						POM						BIS 2012/(WHO, 2011) limits		% of sample exceeding Allowable limit	
	Min.	Max.	Avg.	Median	Std. Dev	Std. error	Min.	Max.	Avg.	Median	Std. Dev	Std. error	Desirable limit	Allowable limit	PRM	POM
U (μg/L)	0.1	28.21	9.56	3.23	4.97	0.53	0.10	24.22	2.12	0.90	4.09	0.44	-	30	–	–
pH	6.71	9.27	7.33	7.24	0.45	0.05	6.65	8.85	7.27	7.35	0.41	0.04	**6.5–8.5**	9.2	1	–
TDS (mg/L)	159	1453	393	326	215.91	23.02	155.40	1674.00	341.80	425.42	284.58	30.34	**600**	1000	3	5
DO	1.49	8.98	3.7	3.03	1.81	0.19	1.58	11.30	3.31	4.0	1.85	0.20	-	-	-	-
Salinity (mg/L)	136	1519	370	298	228.33	24.34	147.54	1591.39	325.87	403.70	270.33	28.82				
EC(μS/cm)	322	2960	801	663	440.46	46.95	316.60	3415.00	699.30	866.32	580.10	61.84	-	1500	6	8
ORP (mV)	−123.5	18.8	−18.7	−12.8	24.87	2.65	−103.9	28.20	−11.75	−14.72	23.66	2.52				
F^- (mg/L)	0.05	3.04	0.41	0.25	0.48	0.05	0.05	4.74	0.21	0.49	0.77	0.08	**1**	1.5	4	4
Cl^- (mg/L)	8.00	449.86	52.74	27.99	62.99	6.72	7.10	717.78	34.49	69.17	101.71	10.84	**250**	1000	–	–
NO_3^- (mg/L)	0.50	86.00	7.01	3.42	10.69	1.14	0.50	73.22	8.97	12.62	12.08	1.29	**45**	–	1	1
SO_4^{2-} (mg/L)	1.00	76.81	17.61	12.30	15.73	1.68	1.00	194.70	12.18	17.81	24.38	2.60	**150**	400	–	–
PO_4^{3-} (mg/L)	0.10	0.14	0.10	0.10	0.01	0.00	0.10	0.23	0.10	0.10	0.02	00	-	-	–	–
TA (mg/L)	30.03	1200.00	265.22	230.20	166.05	17.70	20.00	1311.13	250.11	288.95	178.66	19.05				
HCO_3^- (mg/L)	10.03	1200.00	263.65	230.20	167.97	17.91	0.00	1311.13	250.00	286.45	179.82	19.17	-	**300**	22	26
CO_3^{2-} (mg/L)	0.00	80.00	1.57	0.00	9.69	1.03	0.00	70.00	0.00	2.61	9.62	1.03				
TH (mg/L)	104.00	904.78	238.71	228.00	99.45	10.60	44.04	645.55	178.15	195.96	86.86	9.26	**300**	600	1	1
Ca^{2+} Hardness	38.03	358.31	126.81	124.00	48.82	5.20	24.02	334.29	104.09	119.99	57.03	6.08	**75**	200	3	10
Mg^{2+} hardness	20.00	546.47	111.90	100.00	70.06	7.47	2.00	311.27	62.05	77.00	54.35	5.79	**50**	150	21	7

$$Wi = \frac{wi}{\sum_{i}^{n} wi} \quad (4)$$

$$Qi = \frac{Ci - Cip}{Si - Cip} \times 100 \quad (5)$$

$$SIi = Wi \times Qi \quad (6)$$

$$WQI = \sum_{i-1}^{n} SIi \quad (7)$$

Where wi = weight of the parameters under study; Wi = relative weight; n = no. of parameters; Ci = measured value of each parameter; Cip = value in pure water (taken as 7 for pH and zero for rest of the parameters); Si = standard values for the parameters(WHO, 2011); SIi = sub-index of "*ith*" parameter and Qi = Relative quality value based on concentration of "*ith*" parameter (Adimalla and Qian, 2019).

3.7. *Factor analysis of data multivariate statistical analysis*

The data obtained for water quality parameters were further evaluated by Principal Component Analysis (PCA) using SPSS (version 25) to understand the correlation among the various parameters without loss of any important information.

The data were initially converted into variables termed the principal components wherein the most significant parameters were extracted in the first component, while those with relatively less significance were extracted in the next component and so on.

4. Results and discussion

4.1. *Physicochemical characterization of groundwater - Narmada district*

Various parameters like pH, EC, TDS, total hardness and Ca^{2+}, Mg^{2+}, CO_3^{2-}, HCO_3^-, Cl^-, F^-, NO_3^-, SO_4^{2-} and PO_4^{3-}concentrations were investigated for the water samples under study (Table 2). The ground water was observed to be weakly acidic to alkaline with average pH being 7.33 and 7.22 in PRM and POM seasons respectively and was well within WHO permissible limits of 6.5–8.5 (WHO, 2011).

The mean TDS in groundwater of study area was found to be 393.0 and 341.8 mg/L during PRM and POM seasons respectively. It was observed that 3% and 5% samples during PRM and POM respectively exhibited TDS content above the WHO permissible limit (Table 2) that could be attributed to greater rock-water interactions.

During PRM and POM analysis, Calcium and Magnesium hardness exceeded the desirable limit values in 3%, 10%, and 21%, 7% of samples respectively. Narmada district water was reported to be mixed Ca–Mg–Cl type by Meghana et al. due to rich limestone, dolomite terrains (Patel et al., 2020).

Almost all parameters were within WHO permissible limits except for 5%, 8% and 1% of samples analyzed for fluoride, TDS and nitrate respectively (Table 2).

4.2. *Spatial distribution of some selected parameters in groundwater*

The spatial distribution analysis of all physicochemical parameters as well as Uranium was done with the help of grid map as shown in Fig. 4 (a–k). The grid maps revealed that the majority of study area fell under the permissible limits of WHO for all parameters under study, except for 4% samples for TDS and fluoride, 1% samples for pH, nitrate and sulphate, and 1.5% samples for uranium. It was also observed that some parameters viz; TDS, chloride, nitrate, sulphate, total alkalinity, fluoride and uranium were found higher in Tilakwada tehsil as compared to other tehsils under study [Fig. 4 (a-k circled area)] though concentration of uranium was within AERB permissible limits (AERB and Board, 2004). Fluoride concentrations >1.5 mg/L was also reported by CGWB

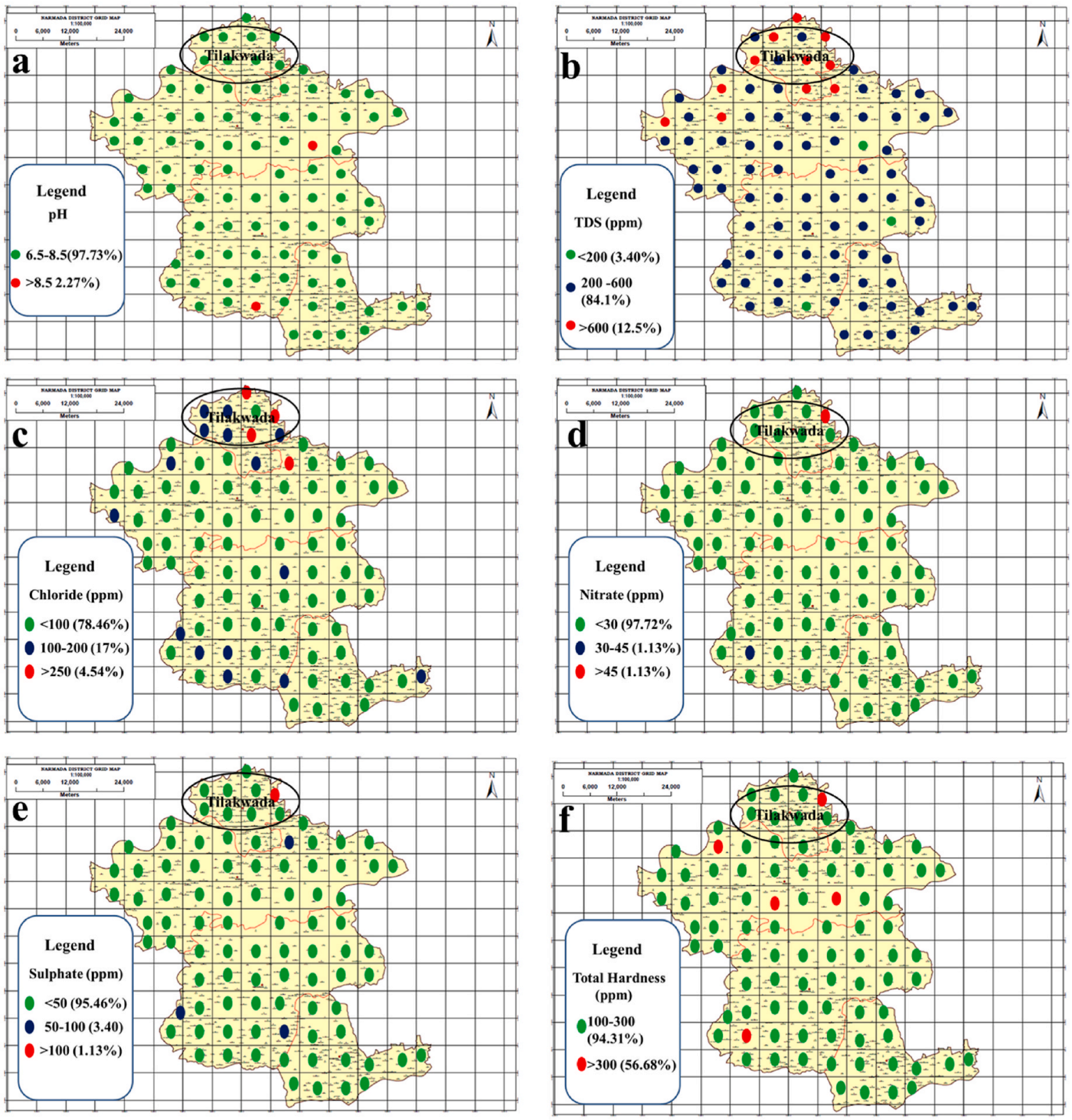

Fig. 4. (a–k) Spatial distribution of pH, TDS, Cl^-, NO_3^-, SO_4^{2-}, Total hardness, Ca Hardness, Mg Hardness, alkalinity, Fluoride and Uranium respectively. Circled area showing the Tilakwada tehsil district, which have slightly higher concentration of above-mentioned parameters.

(CGWB, 2022). The grid maps further indicated that the TDS and chloride concentration increased towards northwest direction in Tilakwada tehsil (Fig. 4 b and c.) with the water being moderately saline while total hardness was reported to be high in Nandod and Dediapada tehsils (Fig. 4f). The rocky terrain and soil porosity might have caused the build up of chloride concentration. Further, Nandod district exhibited spatial variation in TDS, alkalinity and hardness, though within permissible limits, which can be attributed to the presence of shallow depth and permeable alluvial aquifers, making them prone to contamination (Singh et al., 2006). The ground water quality of basaltic aquifers was observed to be of better quality than that of alluvial aquifers. The hardness of water in Nandod and Dediapada tehsils may not pose serious health problems but is recommended to be removed by simple boiling and precipitation. Due to the hydrogeology characteristics of Nandod, careful ground water monitoring and Environment Impact Assessment needs to be performed when any projects are initiated.

The seasonal variations of fluoride were depicted as Box and Whisker plots with outliers (Fig. 5). Significant seasonal and spatial variations were observed for F^-, Cl^-, SO_4^{2-}, Mg-Hardness and total hardness (Amutha et al., 2014) content. Uranium, pH, TDS, F^-, Cl^-, NO_3^-, SO_4^{2-}, total alkalinity, Ca-Hardness, Mg-Hardness and total hardness were observed to have average values of 1.8 μg/L, 7.33, 393 mg/L, 0.41 mg/L, 52.74 mg/L, 7.01 mg/L, 17.61 mg/L, 265.2 mg/L, 126.8 mg/L 111.9 mg/L and 238.7 mg/L in PRM season while in POM season the average values were observed to be 0.90 μg/L, 7.27, 341.80 mg/L, 0.21 mg/L, 34.49 mg/L, 8.97 mg/L, 12.1 mg/L, 104.09 mg/L, 62.00 mg/L and 178.15 mg/L respectively(Fig. 5). The higher values during PRM could be attributed to enhanced evaporation of groundwater during this period (Sahu et al., 2020).

The PRM and POM correlation study indicated a strong correlation of TDS with EC (1), Chloride (0.78), total alkalinity (0.74) and bicarbonate (0.74) and U (0.76) while moderately strong correlation of TDS with

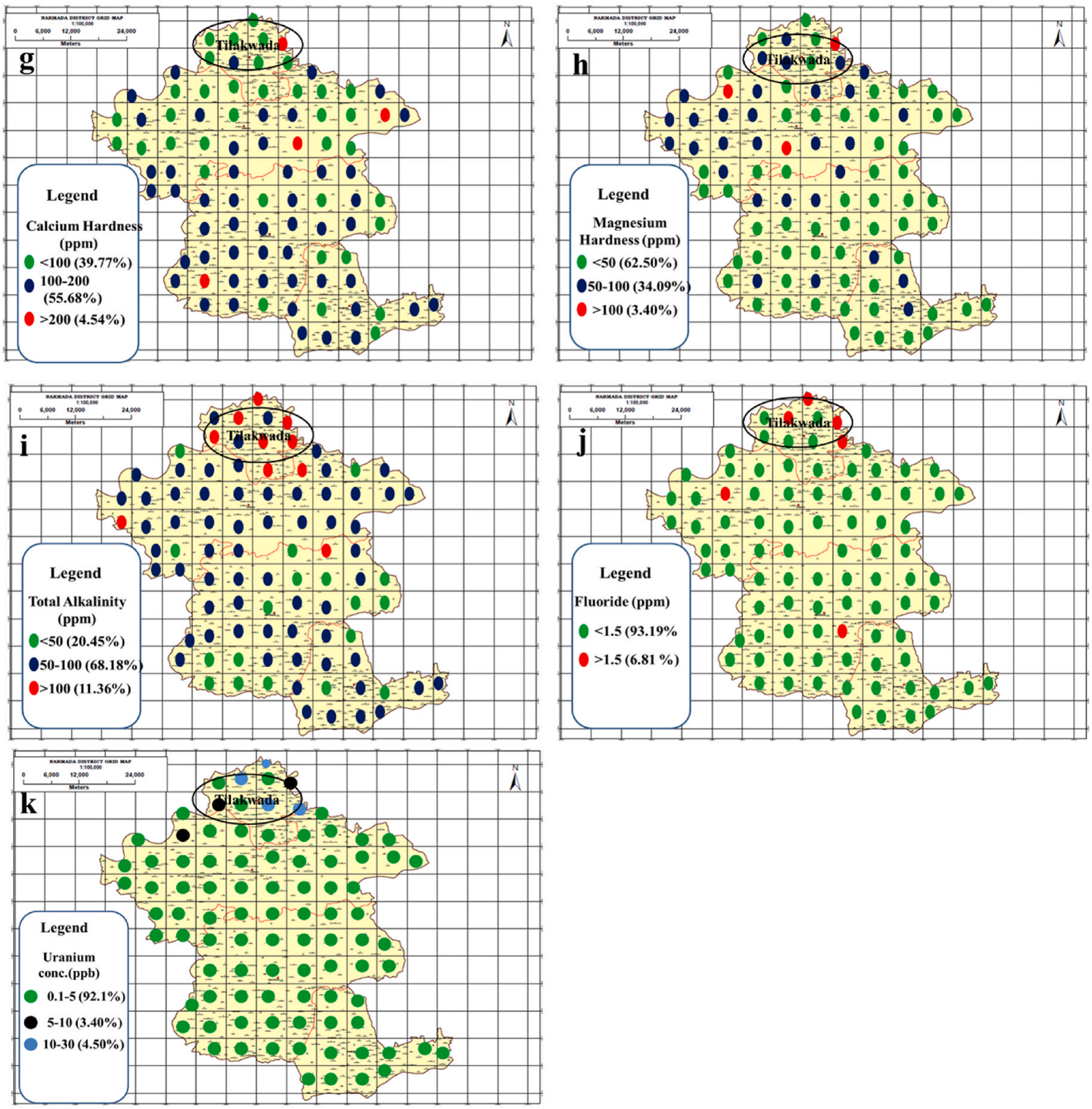

Fig. 4. (*continued*).

fluoride (0.63) was observed indicating that chloride, total alkalinity, bicarbonate, U and fluoride contributed to TDS and EC. Similar correlations in groundwater have been reported (Sharma et al., 2018; Kale et al., 2019). In Tilakwada tehsil the correlation was much more significant and varied as compared to other tehsils of Narmada district (Table 3 a & b), which could be attributed to the varied composition of rocks (CGWB, 2014). It was observed that in Tilakwada tehsil, calcium hardness was positively correlated with chloride, sulphate and nitrate parameters indicating the possible presence of calcium chloride, sulphate and nitrate salts It was observed that uranium was positively correlated with TDS, EC, salinity, chloride suggesting that uranium in groundwater was influenced by the presence of high TDS and chloride (Sharma et al., 2018).

High correlation between EC and TDS indicated presence of large amounts of dissolved salts in water (Selvaraj and Joseph, 2009; Rusydi, 2018). Fluoride exhibited good positive correlation with EC and TDS (r = 0.63). Moderate correlation was observed in Electrical conductivity with sulphate (0.55) and magnesium hardness (0.48) as well as U with total hardness (0.36), Mg hardness (0.5), Total alkalinity (0.74), chloride (0.78) and nitrate (0.51). Fluoride exhibited moderately positive correlation with total alkalinity and HCO_3^-. The basic pH and high concentrations of bicarbonate may be responsible for the solubility of fluoride containing minerals into groundwater (Table 2).

$$CaF_2 + 2\ NaHCO_3 \rightarrow CaCO_3 + 2Na^+ + 2F^- + H_2O + CO_2$$

Positive correlation of uranium with chloride, NO_3^-, total alkalinity and bicarbonate implied that uranium may be present as soluble chlorides, nitrates and bicarbonates (Coyte et al., 2018). Poor correlation of fluoride with nitrate indicated that fluoride is derived from natural sources while the negative correlation of fluoride with Ca^{2+} content may be attributed to the interaction between calcium ion and fluoride ion to form insoluble apatite ($Ca_5(PO_4)_3F$) and fluorite (CaF_2).

4.3. *Groundwater quality assessment for drinking*

The fitness of groundwater for drinking (WQI) was evaluated using equations 2-5. The water was categorized as excellent if WQI< 25; good when WQI ranged from 25 to 50; poor when WQI was in the range 50–75; very poor when WQI ranged from 75 to 100; and unfit for

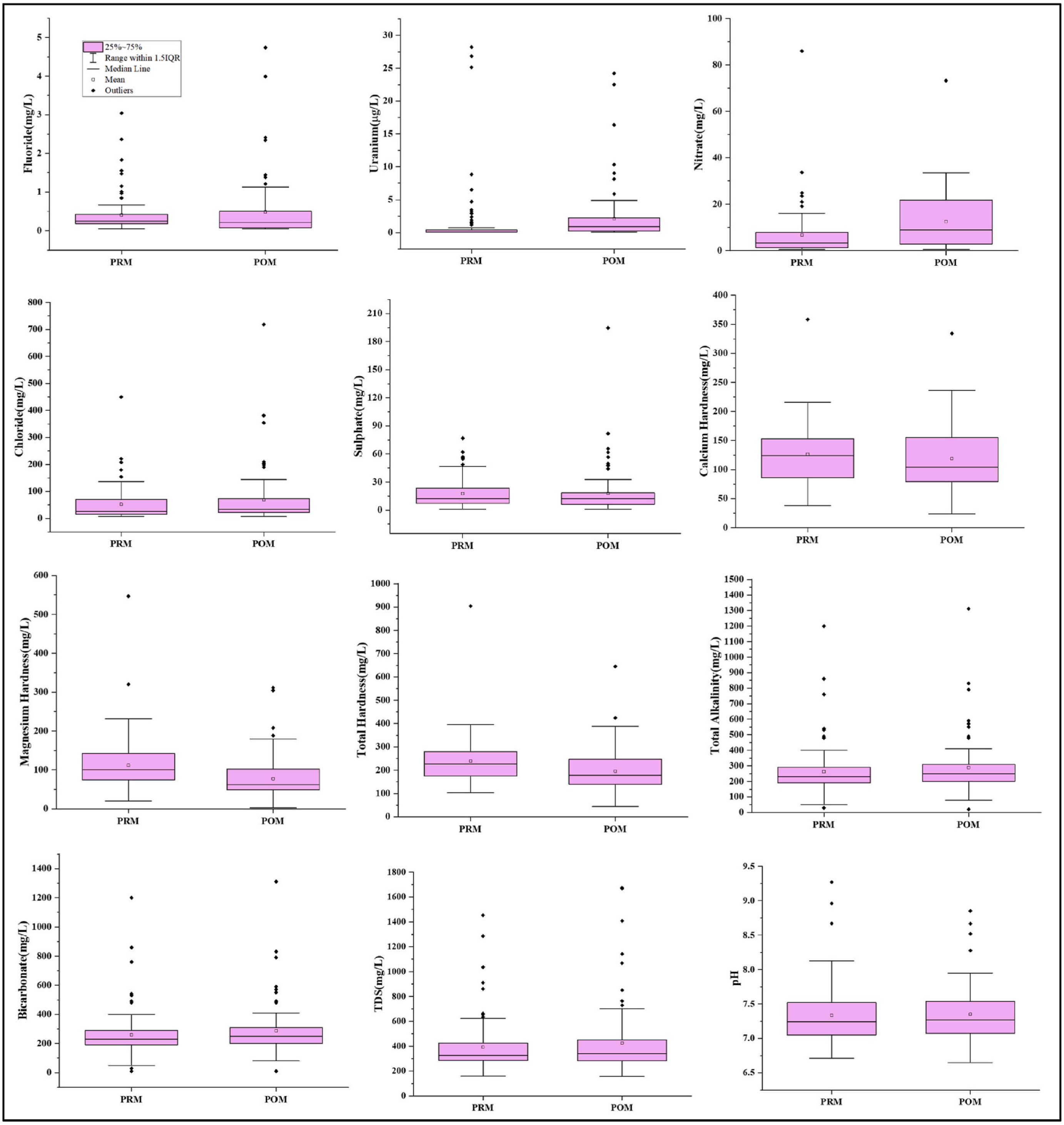

Fig. 5. Box-whisker plot showing fluoride, uranium, nitrate, chloride, sulphate, Ca-hardness, Mg- hardness, total hardness, alkalinity, bicarbonate, total dissolved solids concentration and pH respectively of pre-and post-monsoon data for the Narmada district. The plots depict outliers, median, 75th, and 25th percentile values.

drinking if WQI >100. On the basis of water quality index, the district was divided into 4 parts (4 tehsils) (Table 4). It was observed that Dediapada, Nandod and Sagbara had good water quality while Tilakwada was categorized with poor water quality index. This suggested that the water was not potable in Tilakwada tehsil as the high TDS, chloride and alkalinity values may affect the taste, may cause health problems and scale formation.

4.4. Factor analysis of data

Factor analysis was performed for the data obtained from the analysis of water quality parameters including uranium and fluoride levels during the PRM and POM seasons for 89 samples with the data arranged in a matrix. For factor extraction, the PCA technique was used. The PCA results, including each principal component's eigenvalue, are summarized in Table 5. The complete output data were displayed in the form of scree-plot, with component matrix, factor score, and total variance.

Table 3
(a & b) Karl Pearson Correlation Matrix for the mean data obtained during PRM and POM analysis of ground water in Narmada District
a) Correlation study of parameters for Nandod, Dediapada and Sagbara tehsils.
b) Correlation study of parameters for Tilakwada tehsil.

	pH	TDS	EC	F^-	Cl^-	NO_3^-	SO_4^{2-}	PO_4^{3-}	U	TH	CaH	MgH	TA	Bicarbonate
pH	1.00													
TDS	−0.09	1.00												
EC	−0.08	1.00	1.00											
F^-	0.17	0.14	0.14	1.00										
Cl^-	0.34	0.59	0.59	−0.14	1.00									
NO_3^-	−0.23	0.29	0.29	−0.16	0.28	1.00								
SO_4^{2-}	0.21	0.23	0.23	−0.15	0.75	0.34	1.00							
PO_4^{3-}	−0.09	0.11	0.11	−0.01	0.08	0.04	0.16	1.00						
U	0.01	0.68	0.68	0.08	0.31	0.01	−0.08	0.05	1.00					
TH	−0.47	0.48	0.48	−0.20	0.16	0.41	0.02	0.09	0.37	1.00				
CaH	−0.45	0.14	0.14	−0.23	0.11	0.44	0.25	0.15	−0.16	0.65	1.00			
MgH	−0.24	0.51	0.51	−0.07	0.12	0.16	−0.19	0.00	0.63	0.76	0.01	1.00		
TA	−0.35	0.61	0.61		−0.16	−0.04	−0.40	0.04	0.46	0.45	0.13	0.48	1.00	
Bicarbonate	−0.40	0.59	0.59	0.21	−0.17	−0.02	−0.40	0.04	0.44	0.47	0.16	0.48	1.00	1.00

	pH	TDS	EC	F^-	Cl^-	NO_3^-	SO_4^{2-}	PO_4^{3-}	U	TH	CaH	MgH	TA	Bicarbonate
pH	1.00													
TDS	−0.11	1.00												
EC	−0.11	1.00	1.00											
F^-	0.40	0.63	0.63	1.00										
Cl^-	−0.40	0.78	0.78	0.08	1.00									
NO_3^-	−0.51	0.51	0.51	−0.25	0.87	1.00								
SO_4^{2-}	−0.59	0.55	0.55	−0.17	0.92	0.92	1.00							
PO_4^{3-}	−0.11	−0.21	−0.21	−0.11	−0.28	−0.18	−0.26	1.00						
U	0.27	0.76	0.77	0.66	0.51	0.38	0.35	−0.08	1.00					
TH	−0.54	0.43	0.44	−0.32	0.79	0.97	0.89	−0.02	0.36	1.00				
CaH	−0.61	0.36	0.36	−0.38	0.78	0.95	0.92	0.00	0.27	0.98	1.00			
MgH	−0.46	0.48	0.48	−0.26	0.77	0.96	0.83	−0.04	0.42	0.98	0.93	1.00		
TA	0.32	0.74	0.74	0.94	0.19	−0.17	−0.12	0.00	0.67	−0.22	−0.31	−0.14	1.00	
Bicarbonate	0.32	0.74	0.74	0.94	0.19	−0.17	−0.12	0.00	0.67	−0.22	−0.31	−0.14	1.00	1.00

TH- Total Hardness, CaH- Calcium Hardness, MgH- Magnesium Hardness, TA- Total Alkalinity.

Table 4
WQI of water samples in the study region.

Tehsils	Water Quality Index		Water quality status
	PRM	POM	
Dediapada	21.85	32.65	Excellent in PRM and good in POM
Nandod	35.25	25.75	Good water quality
Sagbara	25.98	17.37	Good in PRM and excellent in POM
Tilakwada	64.68	93.36	Poor quality in PRM and very poor quality in POM

Scree-plots for both seasons exhibited comparable shifts after the third eigenvalue (Fig. 6).

Table 5 shows the extracted rotated and unrotated component eigen values, percentage and cumulative percentage variance attributed for each factor for both seasons. A value of 1 was used as the eigen criteria value for extracting each component. Even though there was less industrial activity and fewer people living in Narmada district, most of the district is covered by mountainous terrain, making geogenic processes the most likely source of groundwater pollution (CGWB, 2014). Factor analysis performed for 14 variables from the sampling region indicated that cumulative extraction of squared loading in the PRM and POM periods to be 84.391% and 83.315% respectively, as shown in Table 5.

According to Table 5, factor 1 was significantly loaded with TDS, EC, hardness, alkalinity, salinity, F^-, Cl^-, NO_3^-, uranium, and HCO_3^- in both seasons (factor score>0.5). Over-usage of groundwater and geogenic sources may be the main cause of these variables in study area. Only nitrate, total hardness, and calcium hardness were positively loaded on the second factor in both seasons. In pre-monsoon, pH and SO_4^{2-} were observed to be positively loaded in the third component whereas in post-monsoon, only pH was positively loaded with 13.90% and 19.94% of variance respectively.

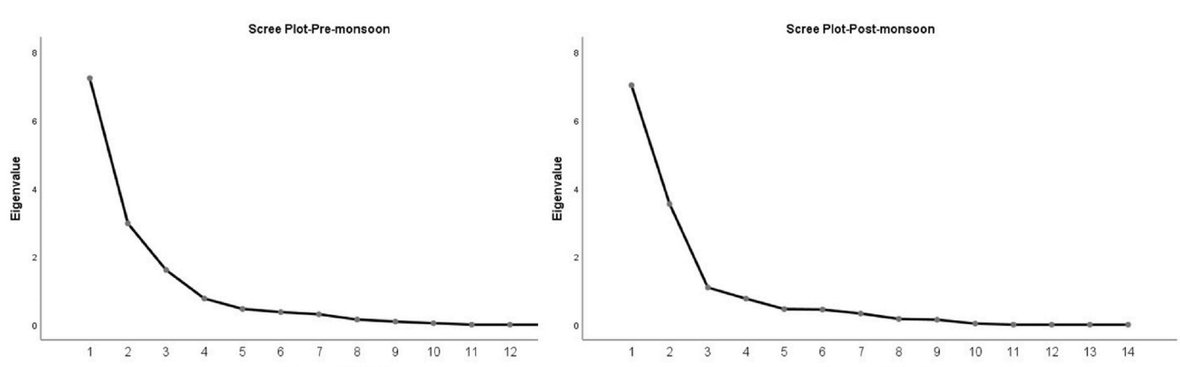

Fig. 6. Scree plot of factor analysis during PRM and POM seasons.

Table 5
Component matrix and extracted factor parameters for study area by PCA.

Variables	Factors[a]					
	PRM			POM		
	1	2	3	1	2	3
pH	−.030	−0.204	**0.795**	0.084	**−0.648**	**0.572**
TDS	**.962**	−0.203	0.05	**0.985**	−0.037	0.036
EC	**.963**	−0.204	0.05	**0.984**	−0.036	0.038
Salinity	**.963**	−0.209	0.054	**0.984**	−0.036	0.038
F^-	**.589**	**−0.647**	0.043	**0.548**	**−0.555**	0.02
Cl^-	**.811**	0.207	0.467	**0.886**	0.19	0.356
NO_3^-	**.673**	**0.579**	0.034	0.377	**0.701**	0.203
SO_4^{2-}	.356	0.48	**0.646**	**0.649**	0.463	**0.487**
U	**.789**	0.158	0.057	**0.779**	−0.431	−0.164
TH	**.640**	**0.668**	−0.299	0.393	**0.845**	−0.192
CaH	.292	**0.769**	−0.165	0.087	**0.846**	−0.163
MgH	**.705**	0.413	−0.31	**0.536**	0.463	−0.136
TA	**.795**	**−0.524**	−0.22	**0.841**	−0.353	−0.346
Bicarbonate	**.794**	**−0.518**	−0.243	**0.839**	−0.34	−0.353
Eigen Values	7.239	2.973	1.603	7.030	3.543	1.090
Variance (%)	51.708	21.233	11.449	50.216	25.310	7.789
Cumulative %	51.708	72.942	84.391	50.216	75.526	83.315
Rotation sum of squared loadings						
Eigen Values	5.844	4.023	1.947	5.647	3.226	2.792
Variance (%)	41.745	28.737	13.908	40.335	23.040	19.940
Cumulative %	41.745	70.483	84.391	40.335	63.374	83.315

Bold values denote significant scores.
[a] 3 components extracted.

5. Conclusion

This study discusses the geospatial distribution and groundwater quality of Narmada district with sandstone, alluvium and basaltic aquifers. The ground water quality is mainly affected by granitic and limestone terrains of the study area and less affected by anthropogenic activities. The basaltic aquifers were observed to have better quality characteristics as compared to alluvial aquifers. The alluvial and basaltic aquifers in Nandod resulted in spatial variation in Nandod due to permeability and shallowness of the aquifers. The average pH, EC, and TDS of the water samples was found to be in the range 6.41–9.06, 319–3187.5 μS/cm and 157.2–1563.5 mg/L respectively. The average fluoride levels as well as chloride, nitrate and sulphate levels during both the seasons were found to be within WHO acceptable limits. The uranium levels during PRM and POM were observed to be in the range 0.1–28.2 and 0.1–24.22 μg/L respectively. The district's drinking/groundwater was safe except Tilakwada tehsil which is suitable for agricultural purposes. Treatment facilities such as reverse osmosis and ion exchange need to be set up to make the water sustainable for drinking in Tilakwada and preferable in Dediapada and Nandod tehsils too, though simple boiling would be sufficient in the latter two tehsils. However, careful ground water monitoring and Environment Impact Assessment is recommended for future projects. The application of PCA on the chemical components of groundwater indicated that the main pollutants brought on by natural phenomena have been eradicated for all parameters. The first component showed a positive correlation with all 14 variables except pH, suggesting geological processes such as weathering of rocks to be the main causative factors.

Declaration of competing interest

The authors declare that they have no known competing financial interests or personal relationships that could have appeared to influence the work reported in this paper.

Data availability

No data was used for the research described in the article.

Acknowledgement

One of the authors Divya Patel acknowledges Board of Research in Nuclear Sciences (BRNS), DAE for financial assistance. The authors acknowledge Department of Chemistry, Faculty of Science, MSU for laboratory facilities.

References

Adimalla, N., Qian, H., 2019. Groundwater quality evaluation using water quality index (WQI) for drinking purposes and human health risk (HHR) assessment in an agricultural region of Nanganur, south India. Ecotoxicol. Environ. Safety. 176, 153–161. https://doi.org/10.1016/j.ecoenv.2019.03.066.
AERB, 2004. In: Board, A.E.R. (Ed.), Limit on Uranium in Drinking Water. Mumbai, India.
Ali, S., Fakhri, Y., Golbini, M., Thakur, S.K., Alinejad, A., Parseh, I., Shekhar, S., Bhattacharya, P., 2019. Concentration of fluoride in groundwater of India: a systematic review, meta-analysis and risk assessment. Groundw. Sustain. Dev. 9, 100224 https://doi.org/10.1016/j.gsd.2019.100224.
Amutha, M., Gubendran, A., Jeyaprabha, B., Periakaruppan, P., 2014. Environmental hydro chemistry and genesis of fluoride in drinking water of govt kallar hr. Sec schools, in dindigul district in tamilnadu India. IOSR Journal of Applied Chemistry 7, 64–71. https://doi.org/10.9790/5736-07616471.
APHA, 2017. Standard Methods for the Examination of Water and Waste Water. American Public Health Associatio, American Water Works Assocition and Water Environment Federation, Washington, DC.
Arulnangai, R., Mohamed Sihabudeen, M., Vivekanand, P.A., Kamaraj, P., 2021. Influence of physico chemical parameters on potability of ground water in ariyalur area of Tamil Nadu, India. Mater. Today Proc. 36, 923–928. https://doi.org/10.1016/j.matpr.2020.07.033.
Balaram, V., Rani, A., Rathore, D.P.S., 2022. Uranium in groundwater in parts of India and world: a comprehensive review of sources, impact to the environment and human health, analytical techniques, and mitigation technologies. Geosystems and Geoenvironment 1, 100043. https://doi.org/10.1016/j.geogeo.2022.100043.
Battaleb-Looie, S., Moore, F., Jafari, H., Jacks, G., Ozsvath, D., 2012. Hydrogeochemical evolution of groundwaters with excess fluoride concentrations from Dashtestan, South of Iran. Environ. Earth Sci. 67, 1173–1182. https://doi.org/10.1007/s12665-012-1560-z.
Bhalara, P.D., Punetha, D., Balasubramanian, K., 2014. A review of potential remediation techniques for uranium(VI) ion retrieval from contaminated aqueous environment. J. Environ. Chem. Eng. 2, 1621–1634. https://doi.org/10.1016/j.jece.2014.06.007.
Bigalke, M., Schwab, L., Rehmus, A., Tondo, P., Flisch, M., 2018. Uranium in agricultural soils and drinking water wells on the Swiss Plateau. Environ. Pollut. 233, 943–951. https://doi.org/10.1016/j.envpol.2017.09.061.
CGWB, 2014. Groundwater Brochure Narmada District. Government of India Ministry of Water Resources.
CGWB, 2022. Ground Water Year Book of Haryana State (2021-2022). Central Ground Water Board Ministry of Water Resources, Central Ground Water Board, Haryana.
Coyte, R.M., Jain, R.C., Srivastava, S.K., Sharma, K.C., Khalil, A., Ma, L., Vengosh, A., 2018. Large-scale uranium contamination of groundwater resources in India. Environ. Sci. Technol. Lett. 5, 341–347. https://doi.org/10.1021/acs.estlett.8b00215.
Hossain, M.I., Bari, M.N., Kafy, A.A., Rahaman, Z.A., Rahman, M.T., 2022. Application of double lifting method for river water irrigation in the water stressed Barind Tract of northwest Bangladesh. Groundw. Sustain. Dev. 18, 100787 https://doi.org/10.1016/j.gsd.2022.100787.
Hossain, M.I., Bari, M.N., Miah, M.S.U., 2021. Opportunities and challenges for implementing managed aquifer recharge models in drought-prone Barind tract, Bangladesh. Appl. Water Sci. 11, 181. https://doi.org/10.1007/s13201-021-01530-1.
Jain, A.K., Chorasia, L., Senthilkumar, M., 2021. Simulation of groundwater flow under the influence of groundwater abstraction in parts of Narmada River basin in Gujarat State, India. Groundw. Sustain. Dev. 12, 100534 https://doi.org/10.1016/j.gsd.2020.100534.
Kafy, A.A., Abdullah Al, F., Raikwar, V., Rakib, A.A., Kona, M.A., Ferdousi, J., 2021. Geospatial approach for developing an integrated water resource management plan in Rajshahi, Bangladesh. Environmental Challenges 4, 100139. https://doi.org/10.1016/j.envc.2021.100139.
Kale, A., Bandela, N., Kulkarni, J., 2019. Assessment of chemo-radiological risk of naturally occurred uranium in groundwater from the Beed district, India. J. Radioanal. Nucl. Chem. 323 https://doi.org/10.1007/s10967-019-06849-3.
Kale, A., Bandela, N., Kulkarni, J., Raut, K., 2020. Factor analysis and spatial distribution of water quality parameters of Aurangabad District, India. Groundw. Sustain. Dev. 10, 100345 https://doi.org/10.1016/j.gsd.2020.100345.
Keesari, T., Pant, D., Roy, A., Sinha, U.K., Jaryal, A., Singh, M., Jain, S.K., 2021. Fluoride geochemistry and exposure risk through groundwater sources in northeastern parts of Rajasthan, India. Arch. Environ. Contam. Toxicol. 80, 294–307. https://doi.org/10.1007/s00244-020-00794-z.
MSME, 2011. Brief Industrial Profile of Narmada District Ahmedabad, Gujarat. MSME – Development Institute Govt. of India.
Patel, D., Pamidimukkala, P., Chakraborty, D., Yadav, A., 2022. Bharuch District, Gujarat, India: factor analysis and geographical distribution of water quality

characteristics. Environ. Nanotechnol. Monit. Manag. 18, 100732 https://doi.org/10.1016/j.enmm.2022.100732.

Patel, M.P., Gami, B., Patel, A., Patel, P., Patel, B., 2020. Climatic and anthropogenic impact on groundwater quality of agriculture dominated areas of southern and central Gujarat, India. Groundw. Sustain. Dev. 10, 100306 https://doi.org/10.1016/j.gsd.2019.100306.

Patil, D., Deshmukh, P., Fursule, R., Patil, P., 2010. Geochemical studies of fluoride and other water quality parameters of ground water in Dhule region Maharashtra, India. J. Nat. Sci. Biol. Med. 1, 9–11. https://doi.org/10.4103/0976-9668.71665.

Patni, K., Pande, C., Pande, A.P., Tewari, G., Joshi, T., 2020. Distribution of naturally occurring uranium and other heavy toxic elements in selected spring water samples of Pithoragarh District, Uttarakhand, India. SN Appl. Sci. 2, 2129. https://doi.org/10.1007/s42452-020-03947-w.

Patra, A.C., Mohapatra, S., Sahoo, S.K., Lenka, P., Dubey, J.S., Tripathi, R.M., Puranik, V. D., 2013. Age-dependent dose and health risk due to intake of uranium in drinking water from Jaduguda, India. Radiat. Prot. Dosim. 155, 210–216. https://doi.org/10.1093/rpd/ncs328.

Pazand, K., 2016. Geochemistry and multivariate statistical analysis for fluoride occurrence in groundwater in the Kuhbanan basin, Central Iran. Model. Earth Syst. Environ. 2, 72. https://doi.org/10.1007/s40808-016-0127-5.

Rusydi, A., 2018. Correlation between conductivity and total dissolved solid in various type of water: a review. IOP Earth Environ. Sci. 118, 012019 https://doi.org/10.1088/1755-1315/118/1/012019.

Sahu, M., Sar, S.K., Baghel, T., Dewangan, R., 2020. Seasonal and geochemical variation of uranium and major ions in groundwater at Kanker district of Chhattisgarh, central India. Groundw. Sustain. Dev. 10, 100330 https://doi.org/10.1016/j.gsd.2020.100330.

Selvaraj, T., Joseph, K., 2009. Correlation between electrical conductivity and total dissolved solids in natural waters. Malaysian J. Sci. 28 https://doi.org/10.22452/mjs.vol28no1.7.

Sharma, T., Sharma, A., Kaur, I., Mahajan, R., Litoria, P., Sahoo, S., Bajwa, B., 2018. Uranium distribution in groundwater and assessment of age dependent radiation dose in Amritsar, Gurdaspur and Pathankot districts of Punjab, India. Chemosphere 219. https://doi.org/10.1016/j.chemosphere.2018.12.039.

Singh, K.P., Malik, A., Mohan, D., Singh, V.K., Sinha, S., 2006. Evaluation of groundwater quality in northern indo-gangetic alluvium region. Environ. Monit. Assess. 112, 211–230. https://doi.org/10.1007/s10661-006-0357-5.

Srivastava, M., Srivastava, P.K., Kumar, D., Kumar, A., 2021. A systematic study of uranium in groundwater and its correlation with other water quality parameters. Water Supply 22, 2478–2492.

Udeshani, W.A.C., Dissanayake, H.M.K.P., Gunatilake, S.K., Chandrajith, R., 2020. Assessment of groundwater quality using water quality index (WQI): a case study of a hard rock terrain in Sri Lanka. Groundw. Sustain. Dev. 11, 100421 https://doi.org/10.1016/j.gsd.2020.100421.

UNSCEAR, 2016. Sources and Effects of Ionizing Radiation, United Nations Scientific Committee on the Effect of Atomic Radiation, Annex D – Biological Effects of Selected Internal Emitters –Uranium. United Nations, New York.

WHO, 2011. Guideline for Drinking Water Quality. World Health Organization, Geneva, Switzerland.